Evolution of MU69
from a binary planetesimal into contact
via Kozai-Lidov oscillations and nebular drag

Wladimir Lyra

New Mexico State University

Funding

NFDAP – 2019
XRP – 2018
XRP - 2016

Next Generation Very Large Array

NRAO - 2017

SPACE TELESCOPE SCIENCE INSTITUTE
Operated for NASA by AURA

HST - 2016

Computational Facilities

New Horizons meeting, Mar 10th, 2020

EVOLUTION OF MU69 FROM A BINARY PLANETESIMAL INTO CONTACT BY KOZAI-LIDOV OSCILLATIONS AND NEBULAR DRAG

WLADIMIR LYRA[1], ANDREW N. YOUDIN[2], ANDERS JOHANSEN[3]

Draft version March 2, 2020

ABSTRACT

The New Horizons flyby of the cold classical Kuiper Belt object MU69 showed it to be a contact binary. The existence of other contact binaries in the 1–10 km range raises the question of how common these bodies are and how they evolved into contact. Here we consider that the pre-contact lobes of MU69 formed as a binary embedded in the Solar nebula, and calculate its subsequent orbital evolution in the presence of gas drag. We find that the sub-Keplerian wind of the disk brings the drag timescales for 10 km bodies to under 1 Myr for quadratic-velocity drag, which is valid in the asteroid belt. In the Kuiper belt, however, the drag is linear with velocity and the effect of the wind cancels out as the angular momentum gained in half an orbit is exactly lost in the other half; the drag timescales for 10 km bodies remain $\gtrsim$ 10 Myr. In this situation we find that a combination of nebular drag and Kozai-Lidov oscillations is a promising channel for collapse. We analytically solve the hierarchical three-body problem with nebular drag and implement it into a Kozai cycles plus tidal friction model. The permanent quadrupoles of the pre-merger lobes make the Kozai oscillations stochastic, and we find that when gas drag is included the shrinking of the semimajor axis more easily allows the stochastic fluctuations to bring the system into contact. Evolution to contact happens very rapidly (within 10^4 yr) in the pure, double-average quadrupole, Kozai region between $\approx 85-95^\circ$, and within 3 Myr in the drag-assisted region beyond it. The synergy between J_2 and gas drag widens the window of contact to 80°–100° initial inclination, over a larger range of semimajor axes than Kozai and J_2 alone. As such, the model predicts a low initial occurrence of binaries in the asteroid belt, and an initial contact binary fraction of about 10% for the cold classicals in the Kuiper belt. The speed at contact is the orbital velocity; if contact happens at pericenter at high eccentricity, it deviates from the escape velocity only because of the oblateness, independently of the semimajor axis. For MU69, the oblateness leads to a 30% decrease in contact velocity with respect to the escape velocity, the latter scaling with the square root of the density. For mean densities in the range 0.3-0.5 g cm^{-3}, the contact velocity should be $3.3-4.2$ m s^{-1}, in line with the observational evidence from the lack of deformation features and estimate of the tensile strength.

[astro-ph.EP] 2 Mar 2020

Effect of Drag

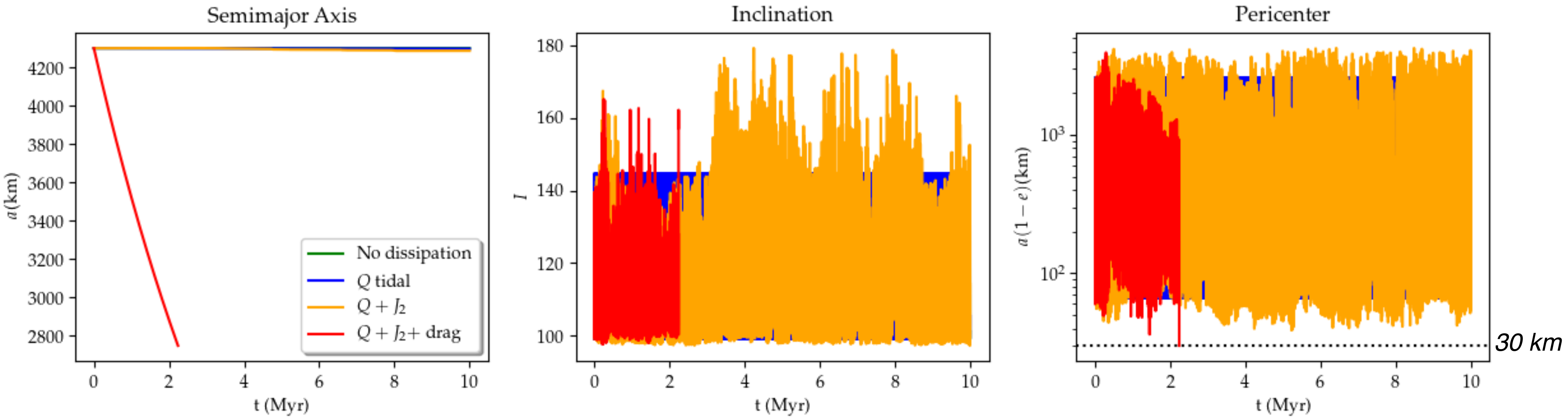

Lyra, Youdin, & Johansen 2020 (submitted)

The Cartoon Image

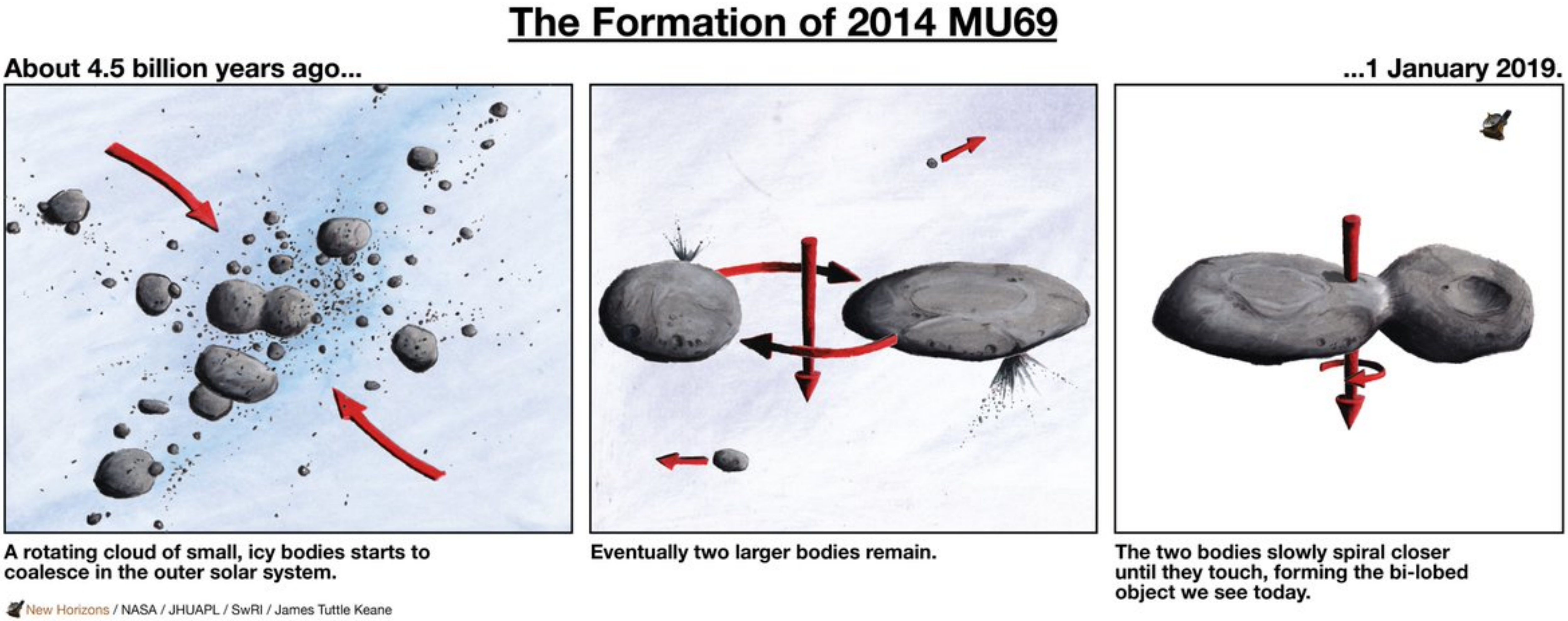

Sketch by J.T. Keane

Beyond the cartoon image

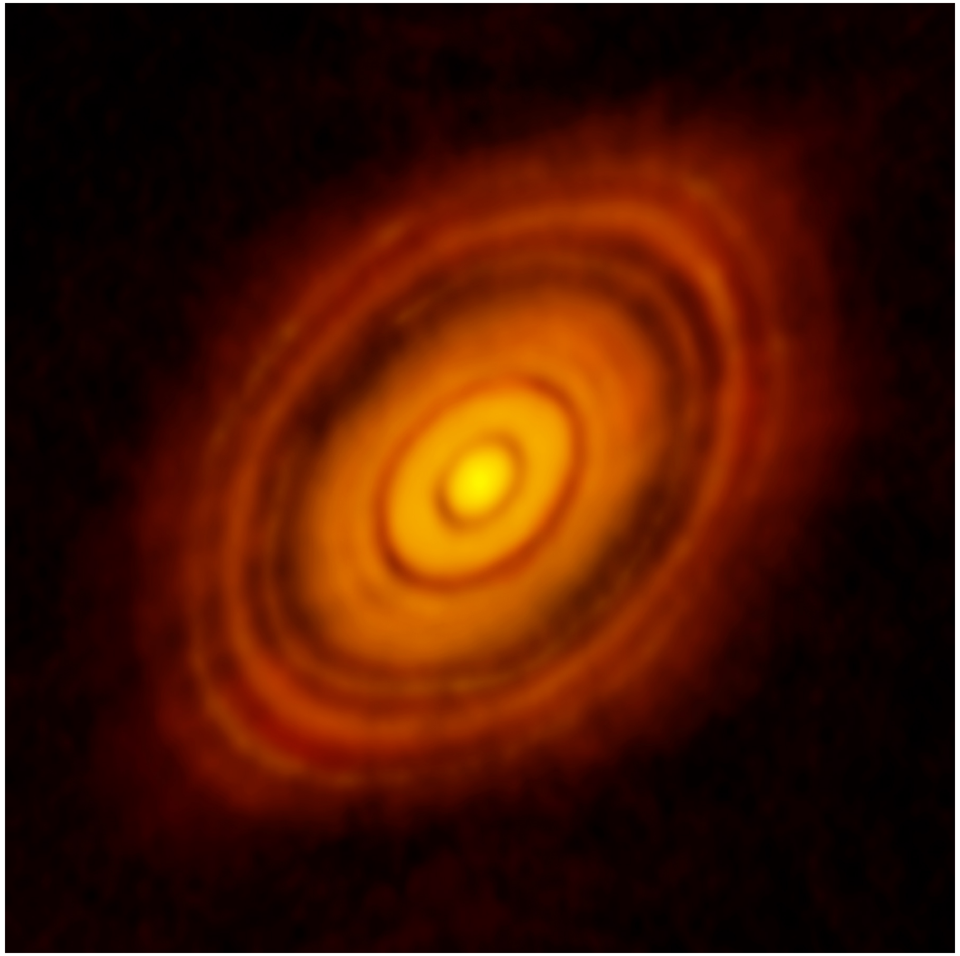

How?

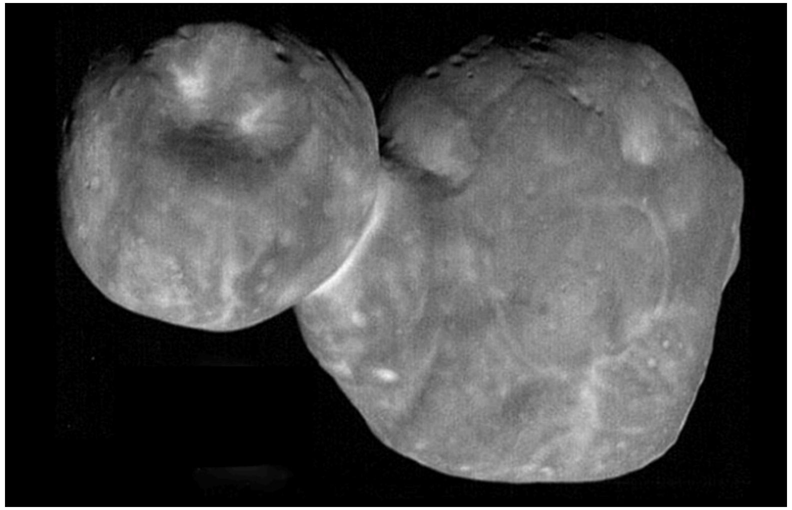

Streaming Instability

The dust drift is hydrodynamically unstable

Youdin & Goodman (2005), Johansen & Youdin (2007)

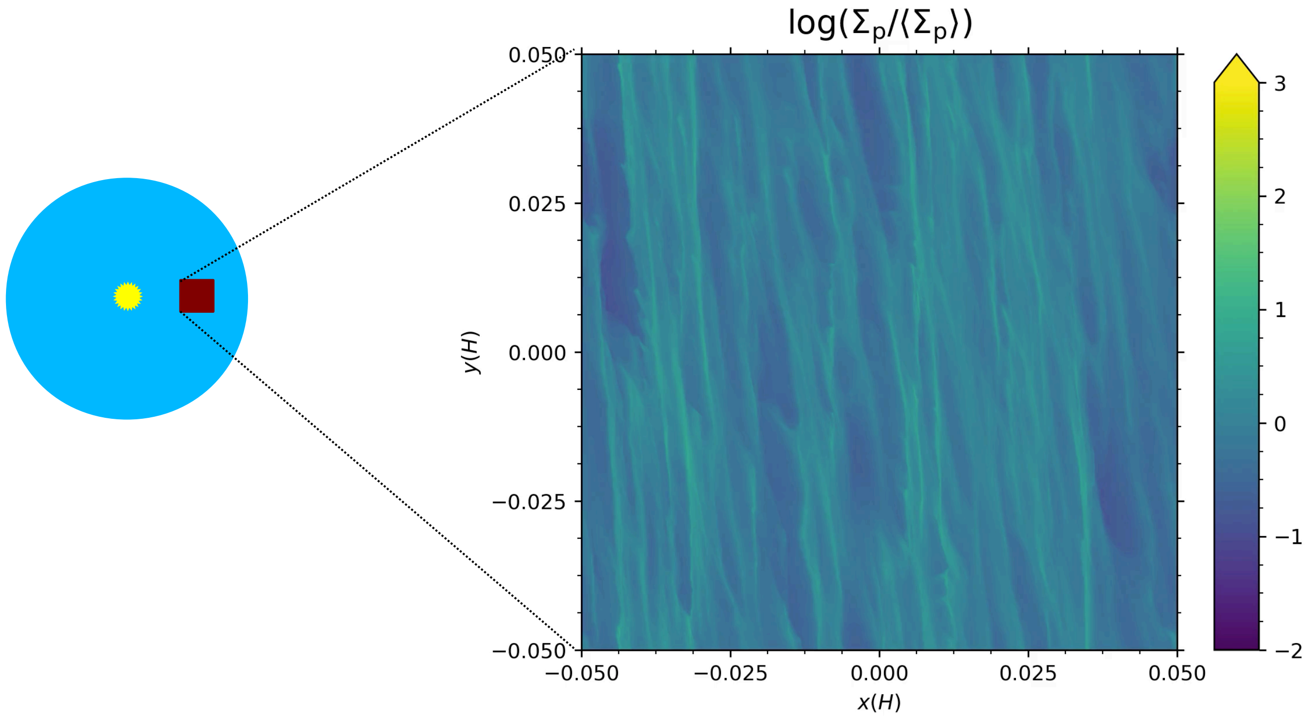

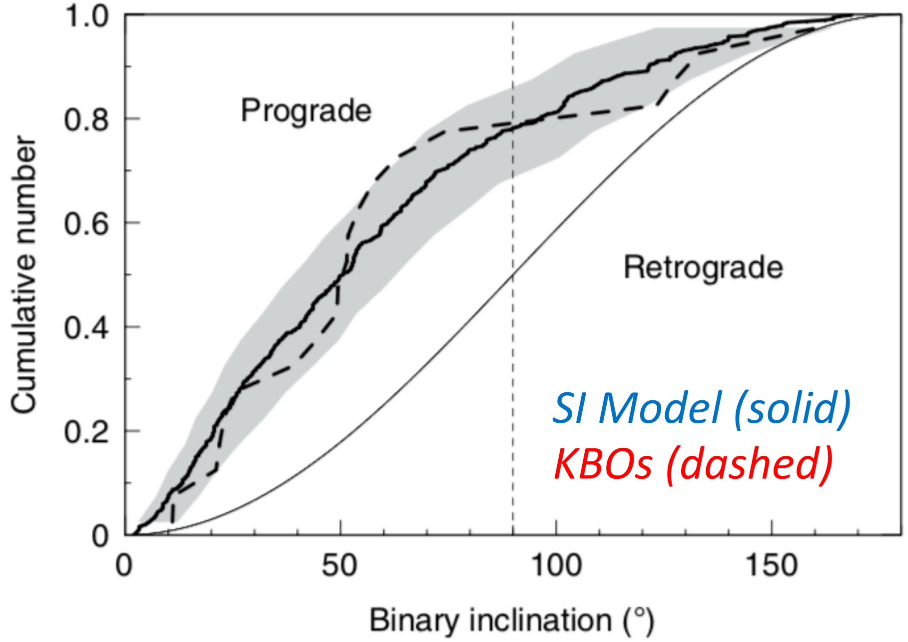

Streaming Instability reproduces the prograde/retrograde distribution of KBO binaries

Nesvorny+'19

Hardening

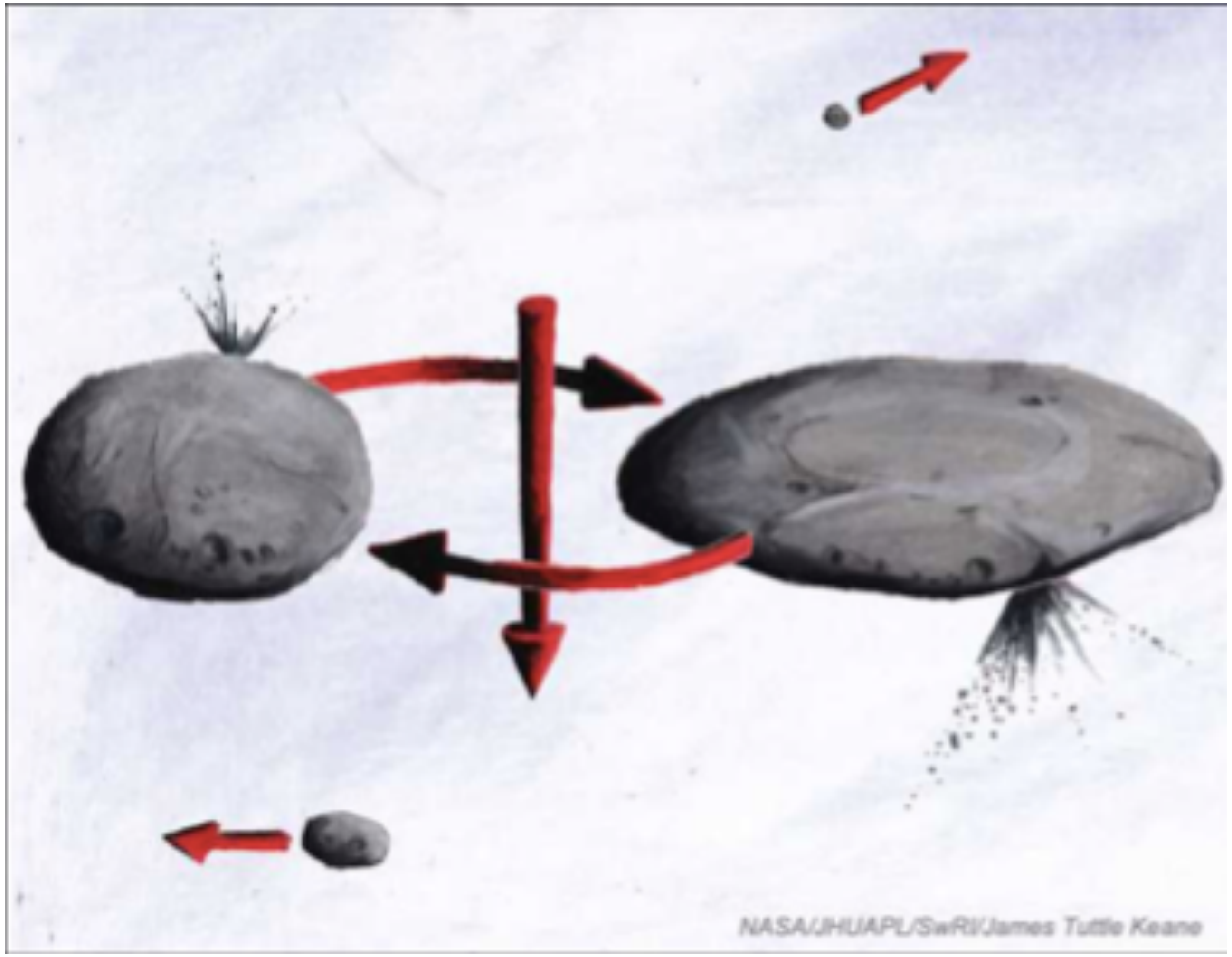

Sketch by J.T. Keane

How was angular momentum lost?

Mutual orbit
(i.e., not captured)

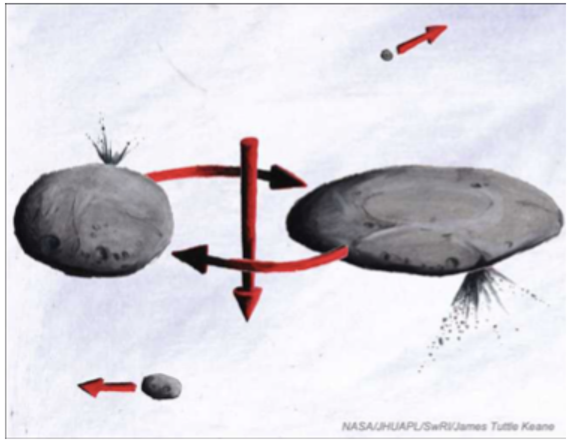

Inferred from:
Alignment of components' axes;
Similar colors.

Sketch by J.T. Keane

Slow merger
(~< 5 m/s)

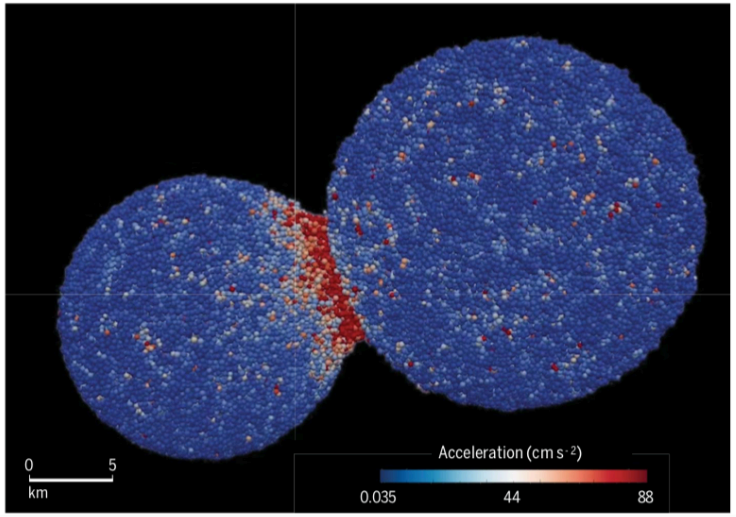

McKinnon et al. (2020)

Inferred from:
Negligible evidence for impact damage
SPH simulations

Angular momentum loss via nebular drag

gravity

drag

$$\ddot{\boldsymbol{r}}_1 = -Gm_2 \frac{(\boldsymbol{r}_1 - \boldsymbol{r}_2)}{|\boldsymbol{r}_1 - \boldsymbol{r}_2|^3} - \frac{\dot{\boldsymbol{r}}_1}{\tau_1}$$

$$\ddot{\boldsymbol{r}}_2 = -Gm_1 \frac{(\boldsymbol{r}_2 - \boldsymbol{r}_1)}{|\boldsymbol{r}_1 - \boldsymbol{r}_2|^3} - \frac{\dot{\boldsymbol{r}}_2}{\tau_2}$$

Solve for angular momentum:

$$r\ddot{\phi} + 2\dot{r}\dot{\phi} = -\frac{r\dot{\phi}}{\tau}$$

$$\frac{dh}{dt} = -\frac{h}{\tau}$$

Exponential decay of angular momentum !

$$h = h_0 e^{-t/\tau}$$

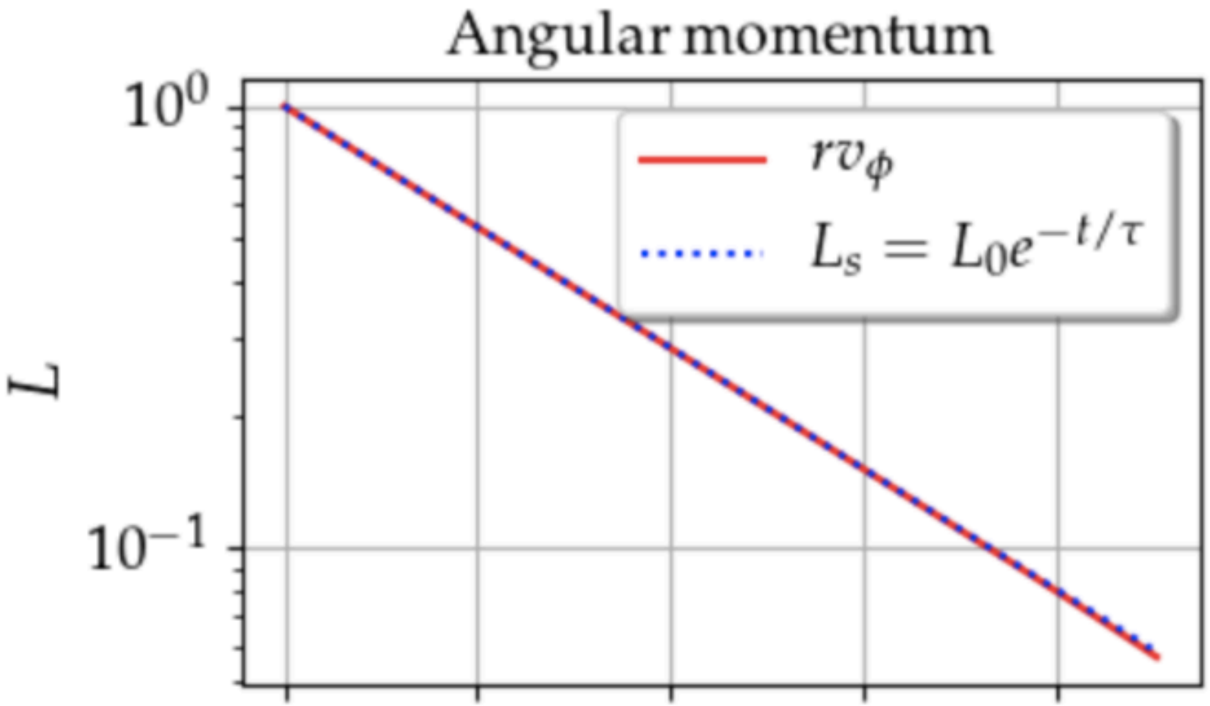

W. Lyra

Lyra, Youdin, & Johansen 2020 (submitted)

Analytical solution

Exponential decay of angular momentum

$$h = h_0 e^{-t/\tau_{\rm eff}}$$

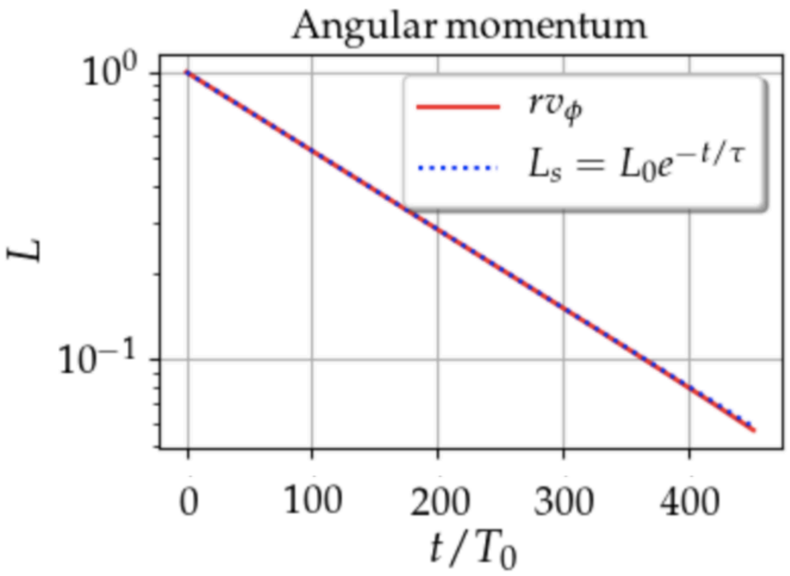

Exponential decay of energy

$$a = a_0\, e^{-2t/\tau_{\rm eff}}$$

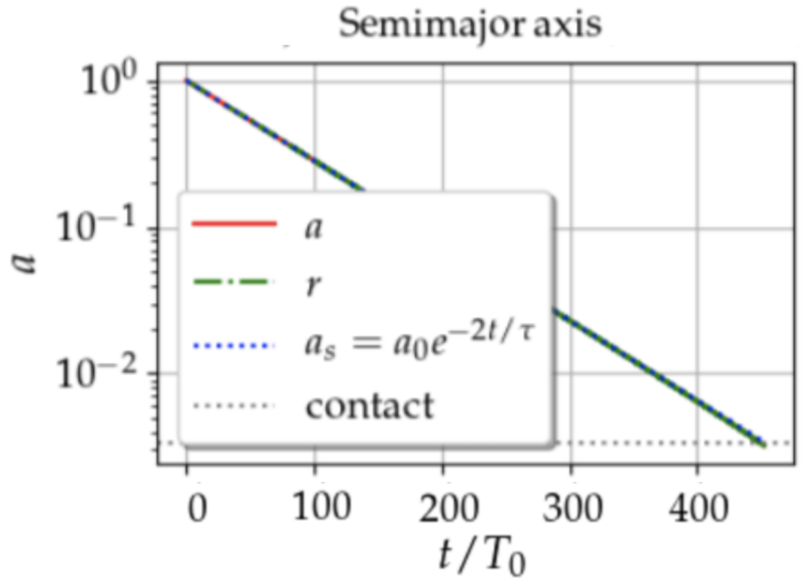

Exponential increase of orbital velocity

$$v_\phi = v_{\phi,0}\, e^{t/\tau_{\rm eff}}$$

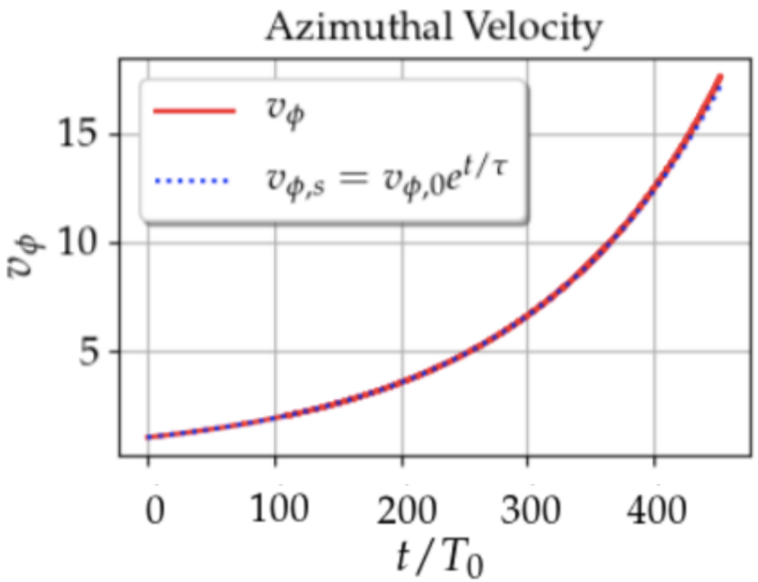

W. Lyra

Lyra, Youdin, & Johansen 2020 (submitted)

Getting quantitative…

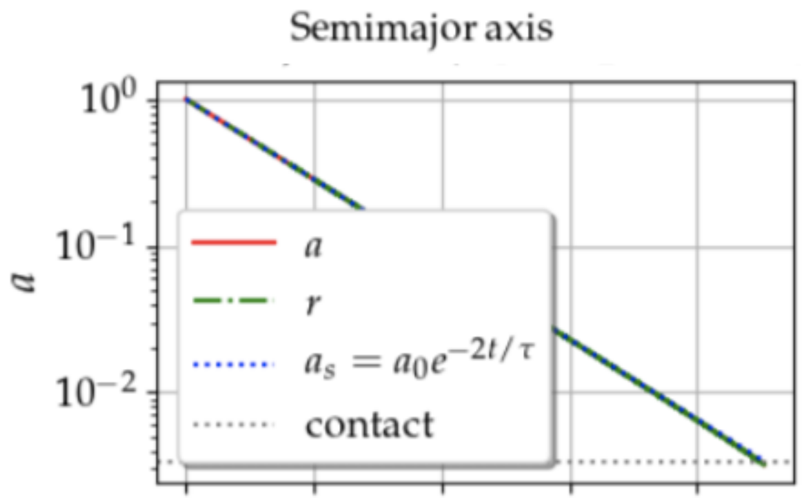

Time until contact

$$t = \frac{\tau}{2} \ln \frac{a_0}{a}$$

For $a = 0.1\, r_H$ (4000 km), hardening to a_0=20km and $\tau\Omega$=10^7 …

t ~ 100 Myr

W. Lyra

Lyra, Youdin, & Johansen 2020 (submitted)

Wind

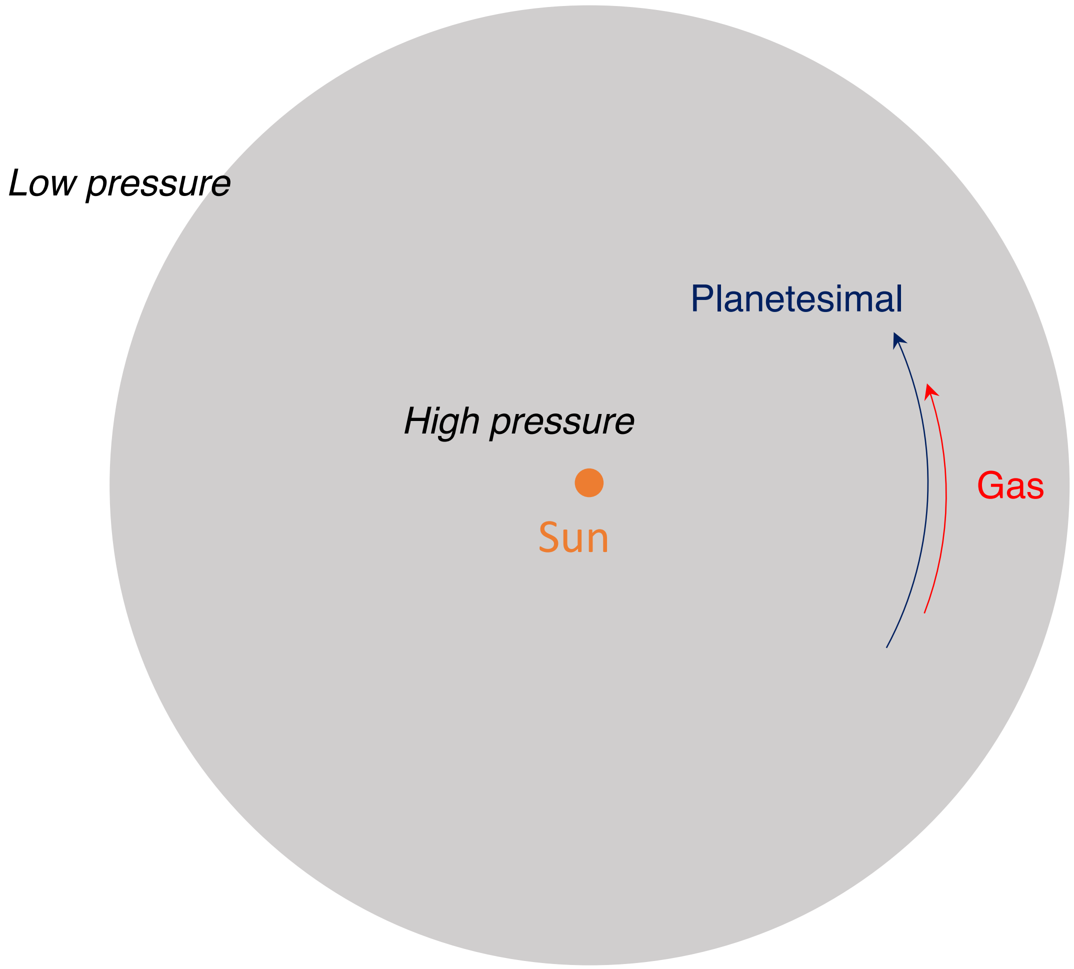

The gas has some pressure support.

The planetesimal has none.

Wind

At initial separation $a \sim$ 4000 km:

Binary orbital velocity **~ 0.1 m/s**

Solar orbit velocity at 45AU
$v_k \sim$ 4.5 km/s

Sub-Keplerian pressure support
$v = v_k (1-\eta)$
$\eta \sim 0.01$

Headwind velocity (v_k-v):
$\eta v \sim$ 50 m/s

Subkeplerian wind on the binary
= 500 times orbital velocity

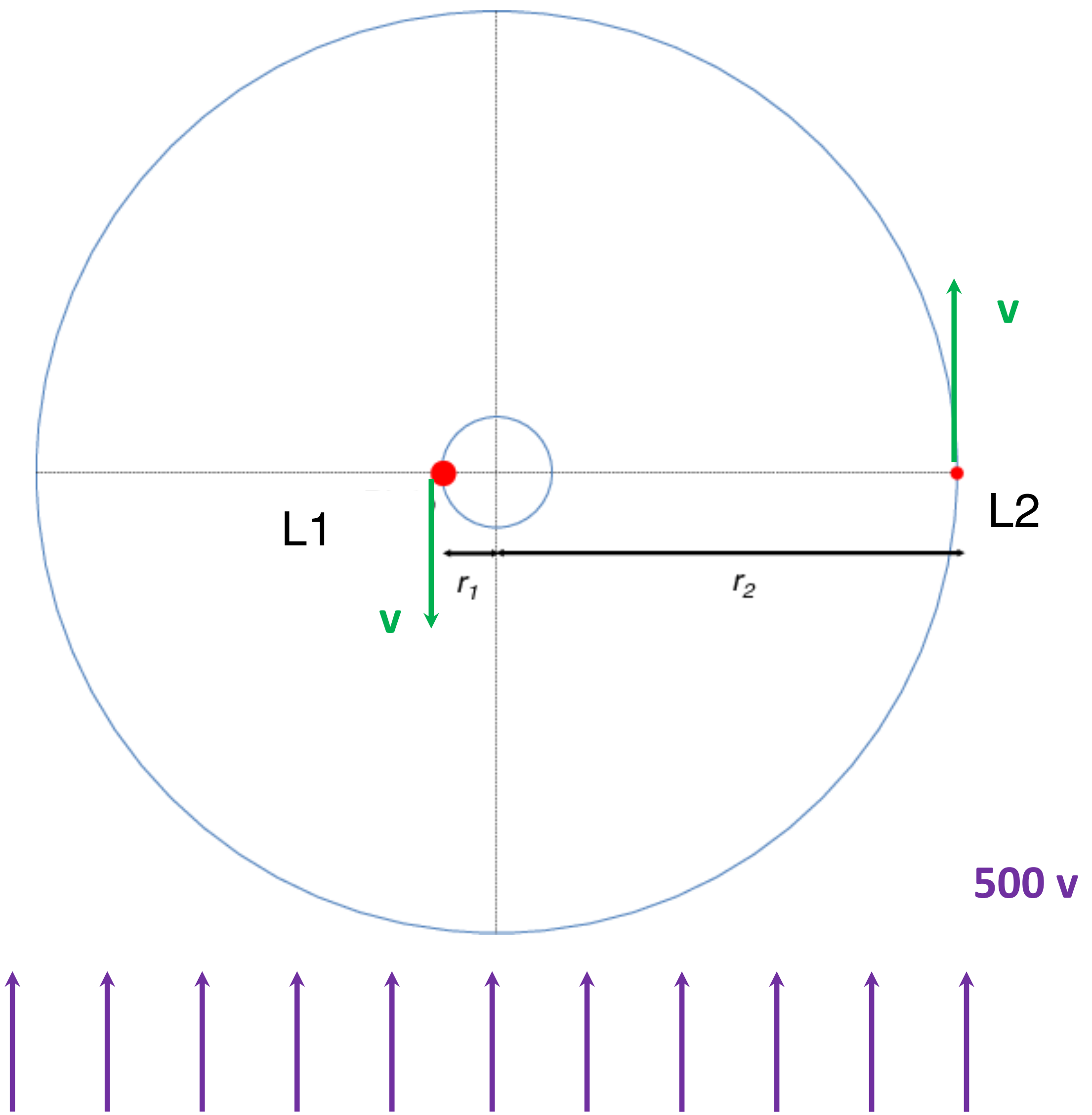

W. Lyra

Lyra, Youdin, & Johansen 2020 (submitted)

Wind solution

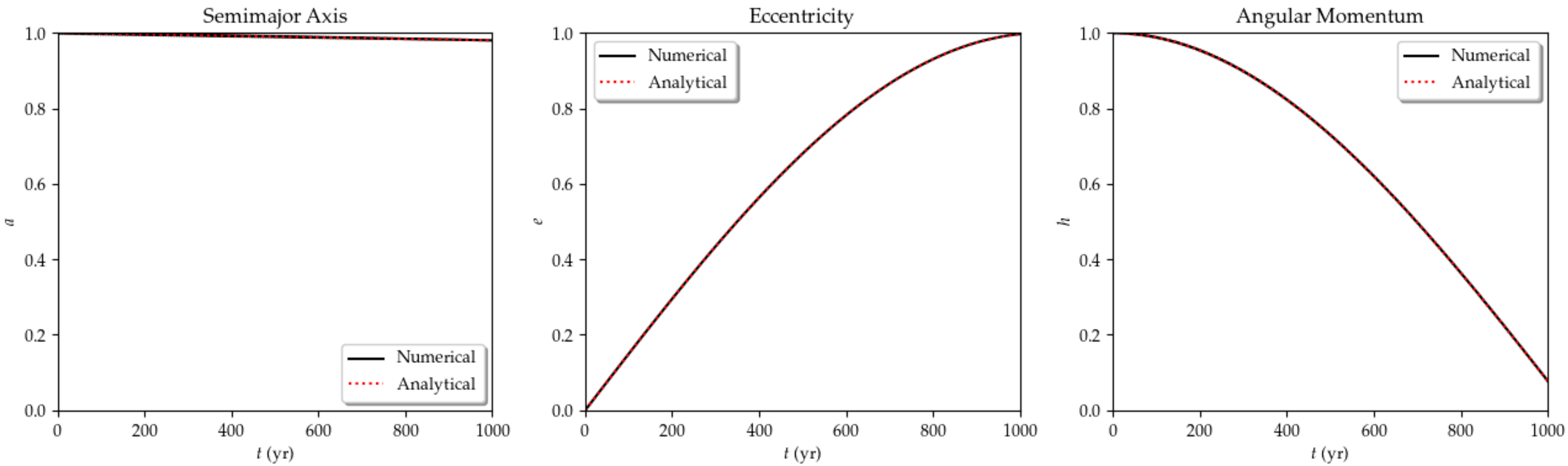

Lyra, Youdin, & Johansen 2020 (submitted)

Wind solution

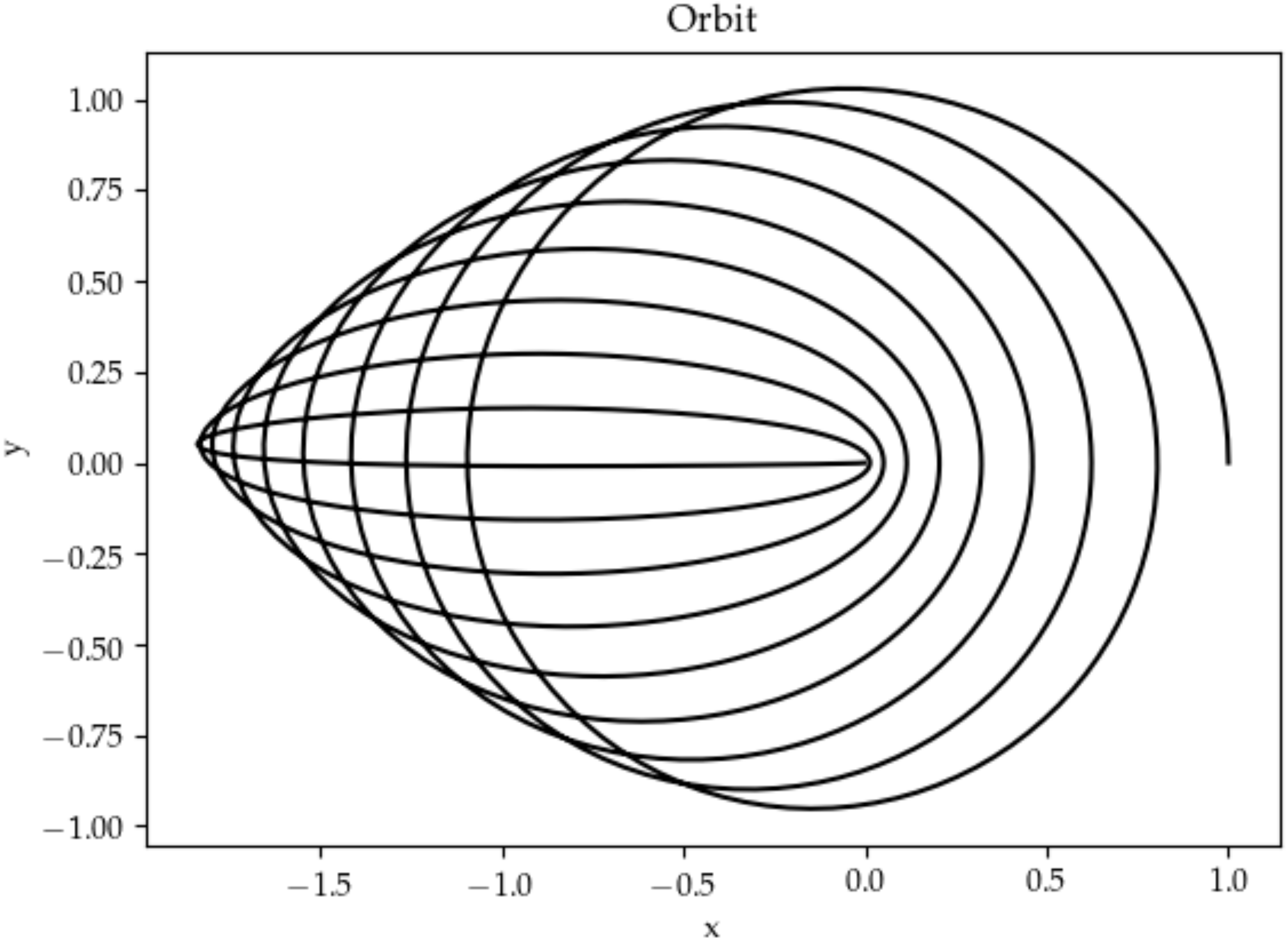

Angular momentum loss at constant energy.

Eccentricity increase at constant semimajor axis

Lyra, Youdin, & Johansen 2020 (submitted)

Timescales

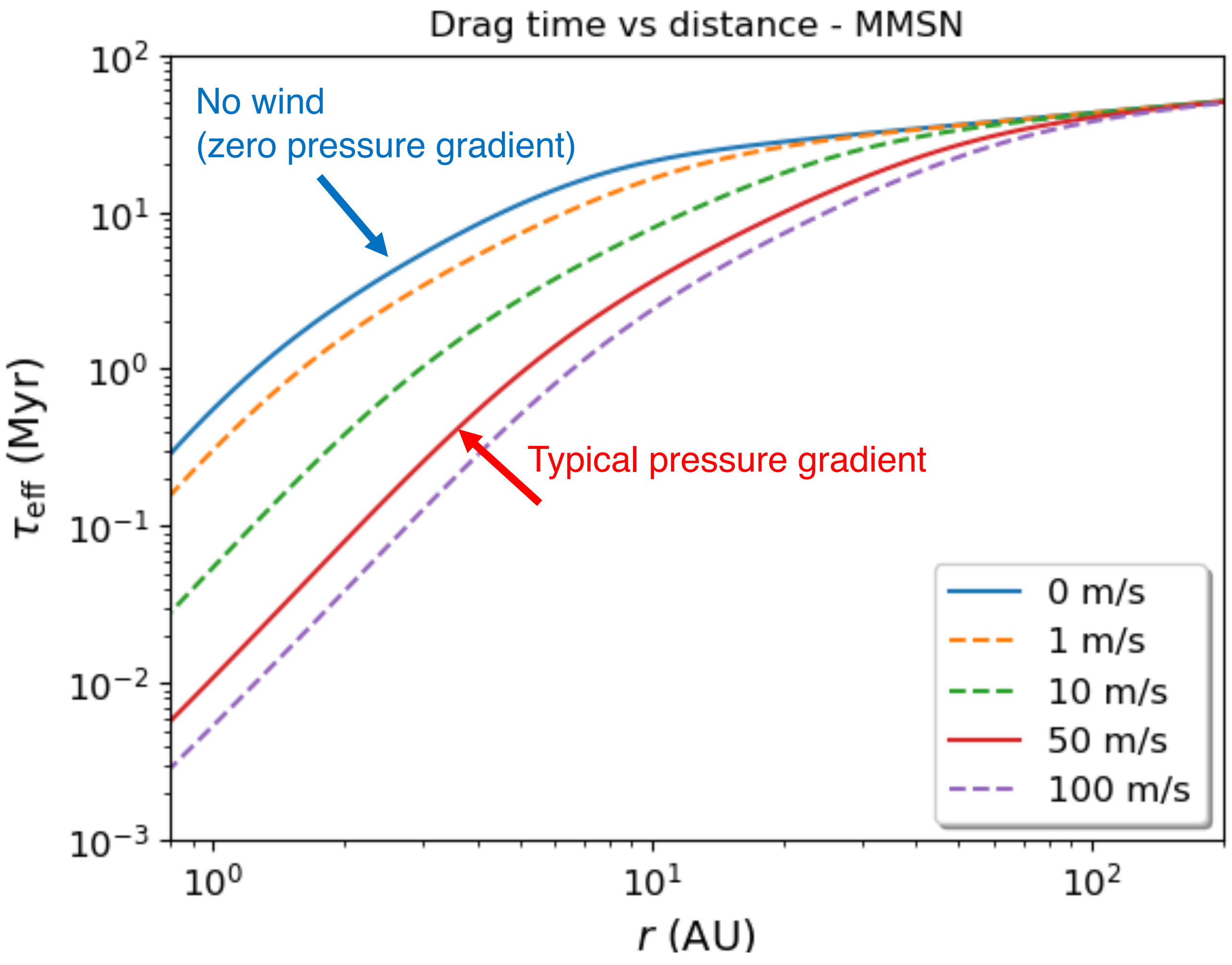

Wind has a strong effect in the distances of the asteroid belt.

Little effect in the Kuiper belt.

Lyra, Youdin, & Johansen 2020 (submitted)

Linear vs quadratic drag

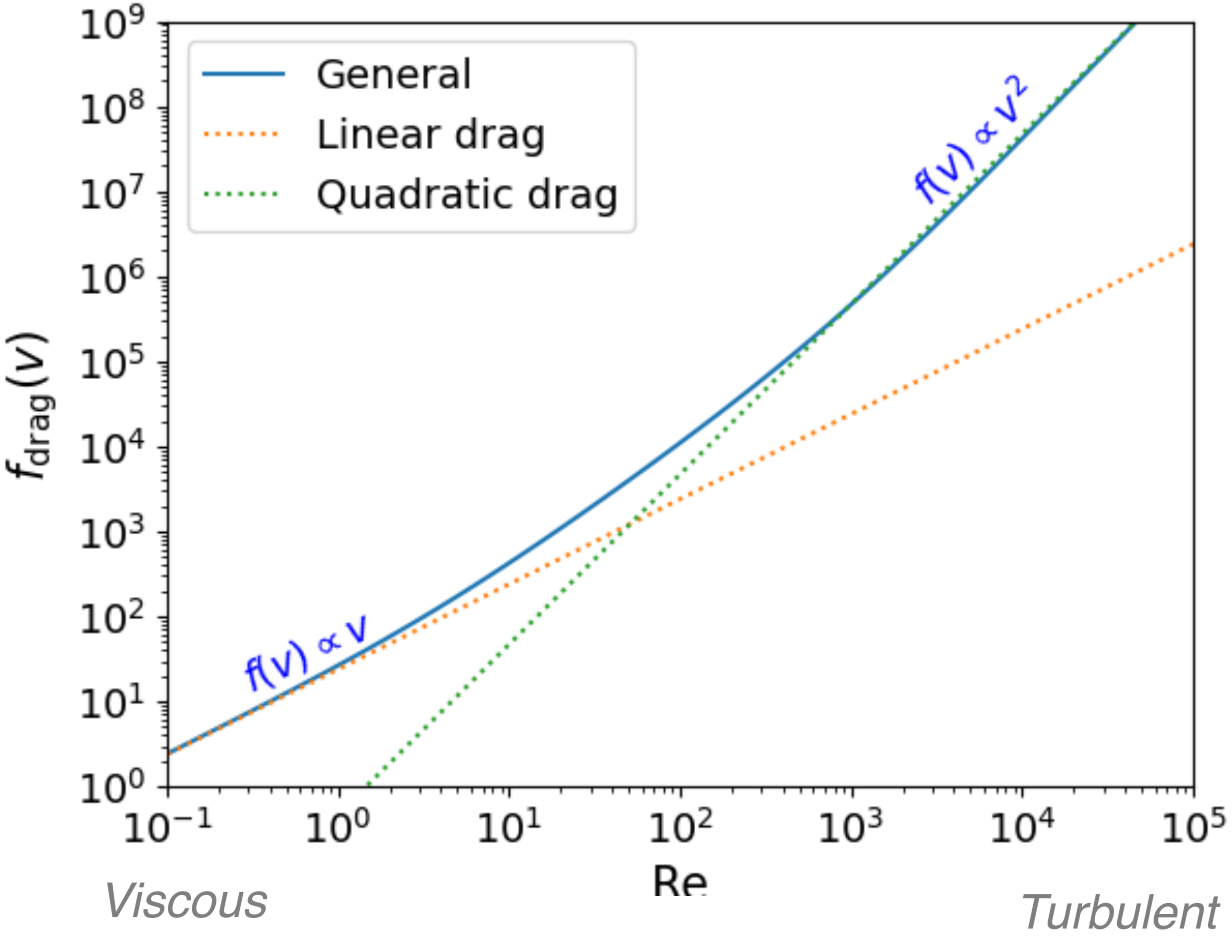

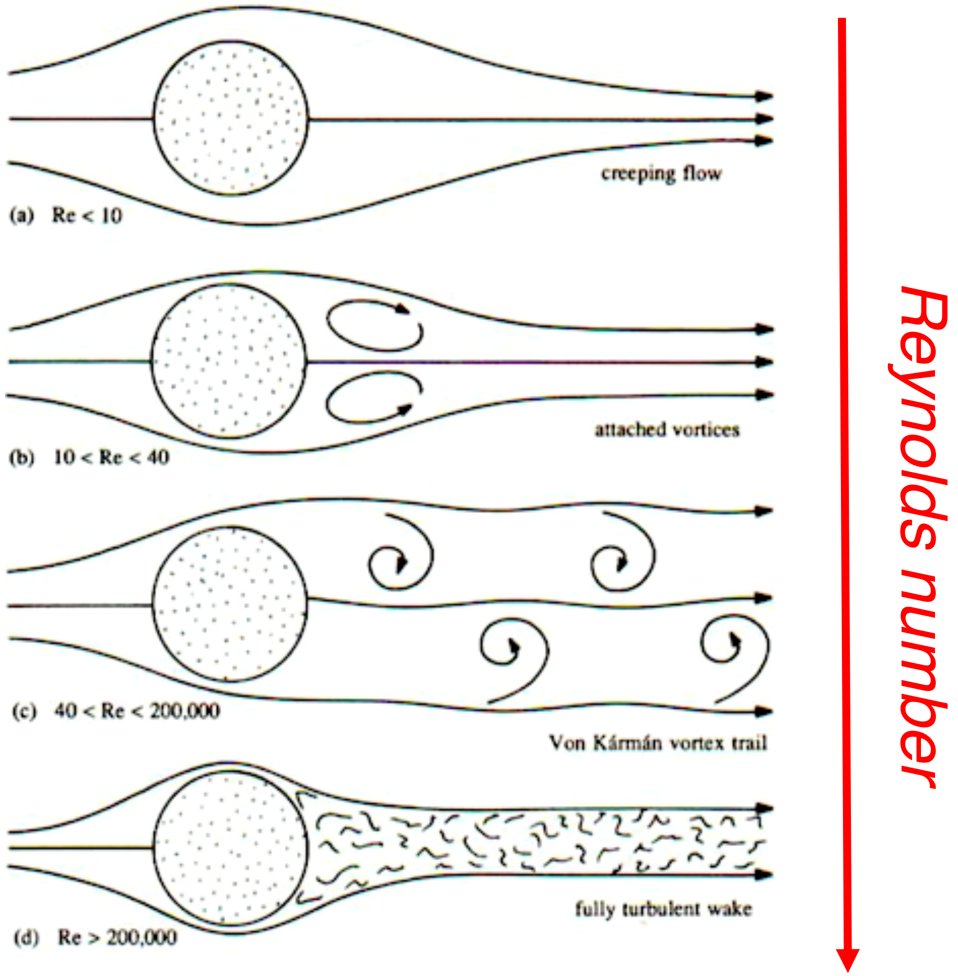

Lyra, Youdin, & Johansen 2020 (submitted)

Linear vs quadratic drag

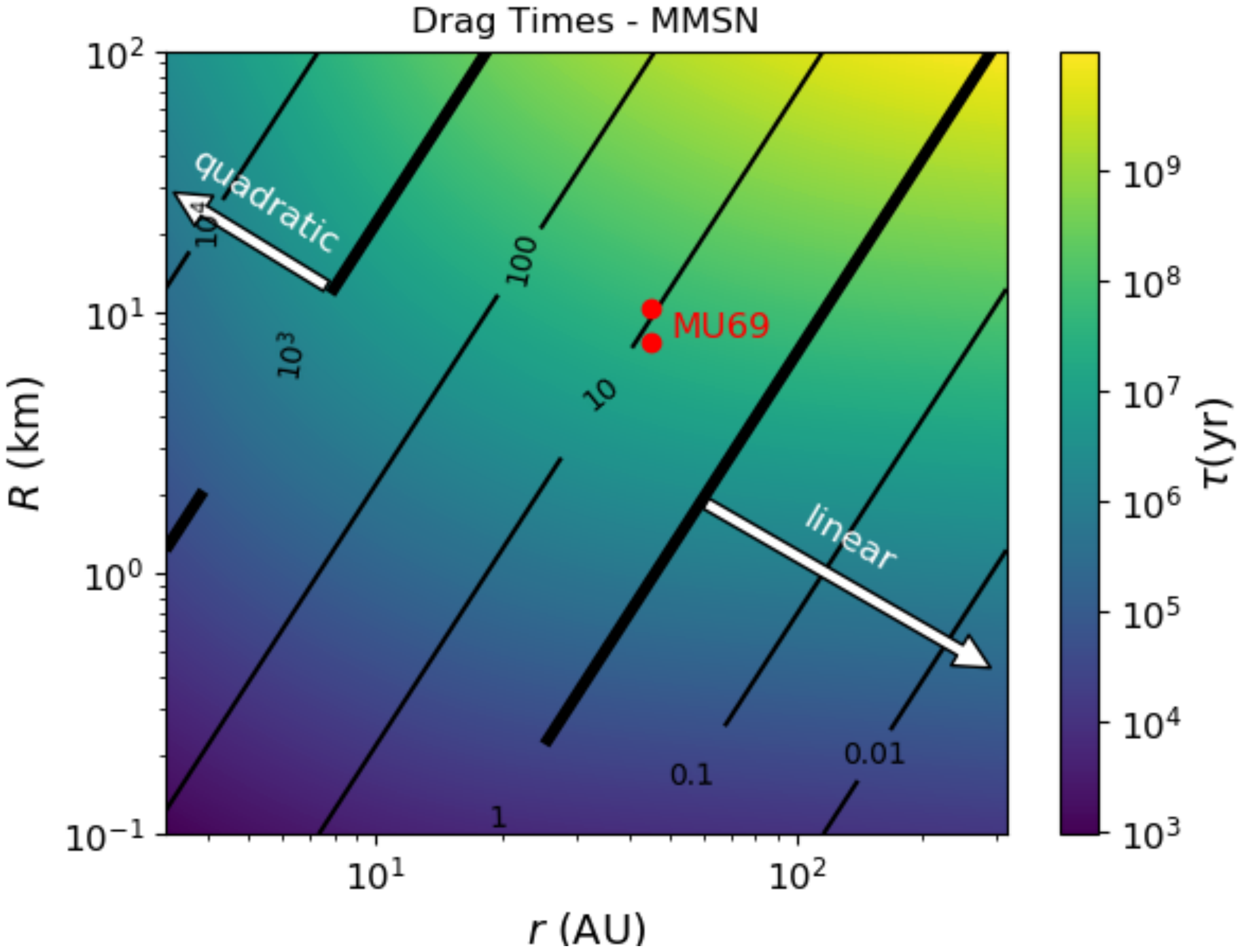

Lyra, Youdin, & Johansen 2020 (submitted)

Effect of Inclination

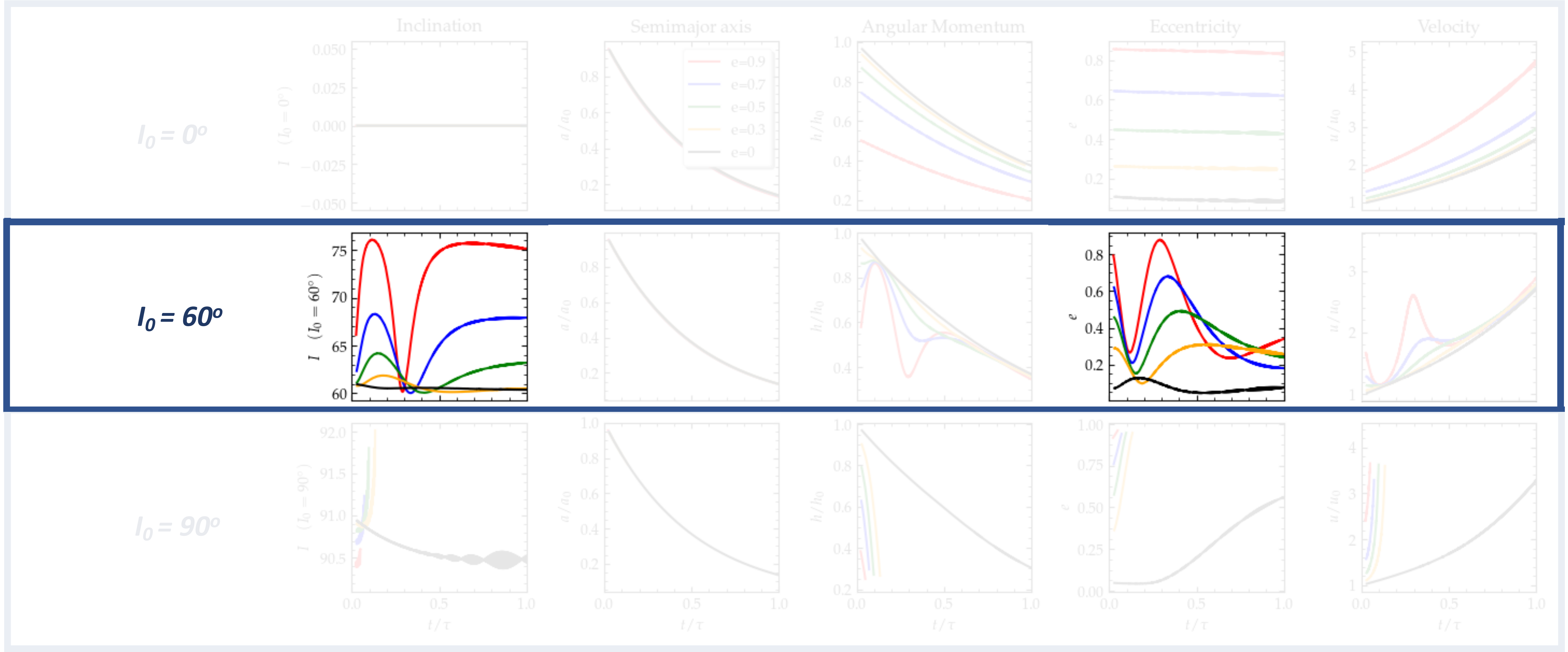

Lyra, Youdin, & Johansen 2020 (submitted)

Kozai-Lidov Oscillations

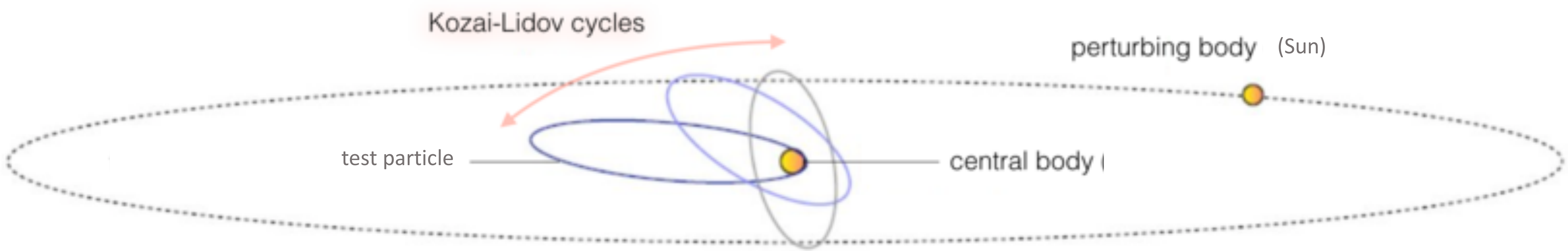

Effect of Inclination

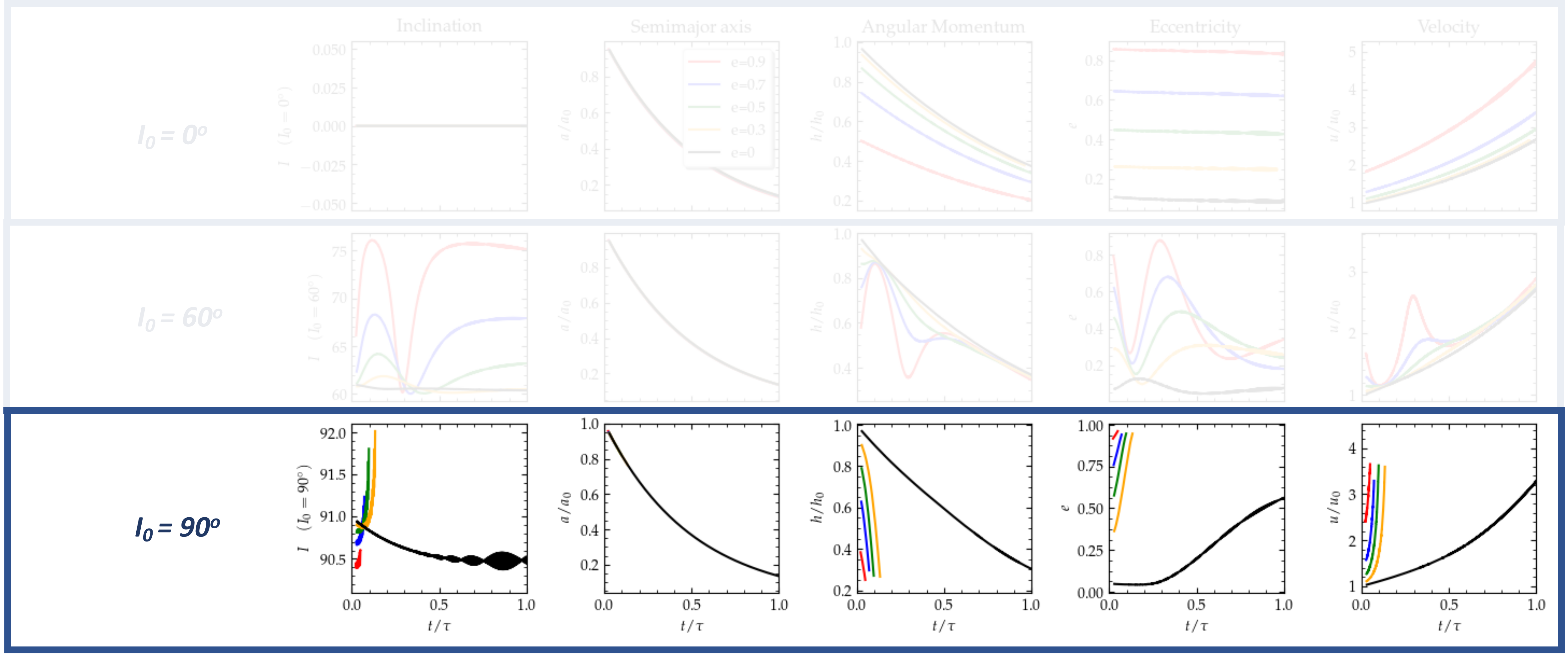

Lyra, Youdin, & Johansen 2020 (submitted)

Kozai + Tidal Friction + Drag

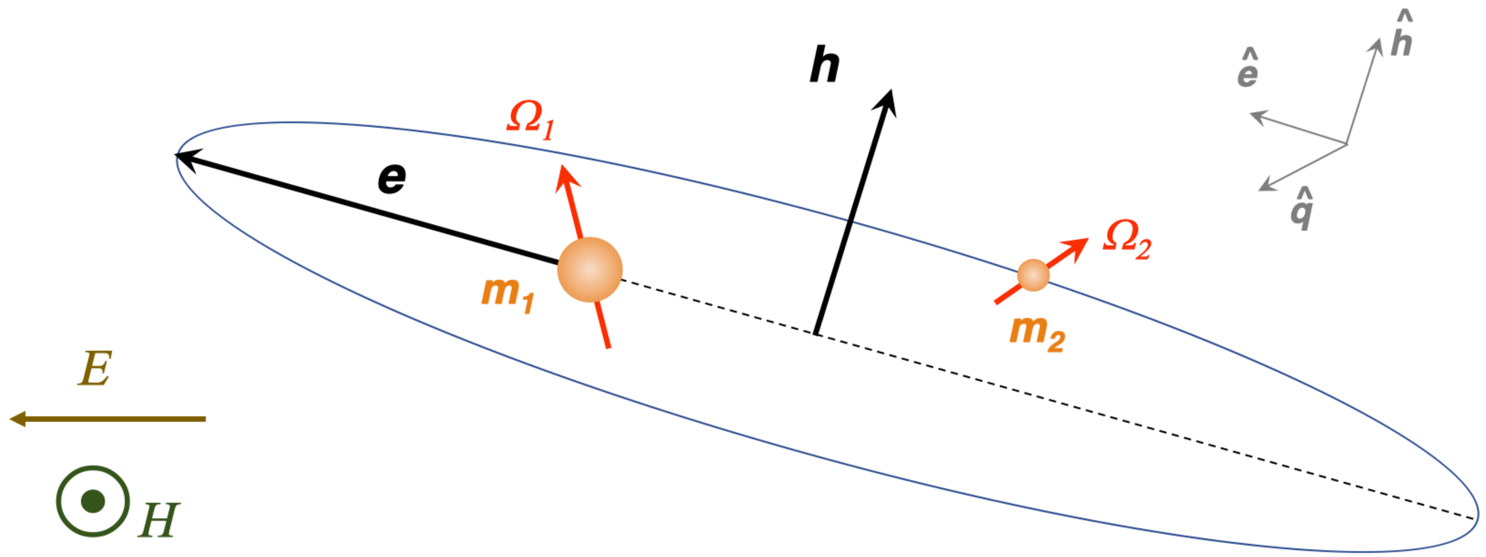

Lyra, Youdin, & Johansen 2020 (submitted)

Critical Inclination

- Contact
- ○ No contact

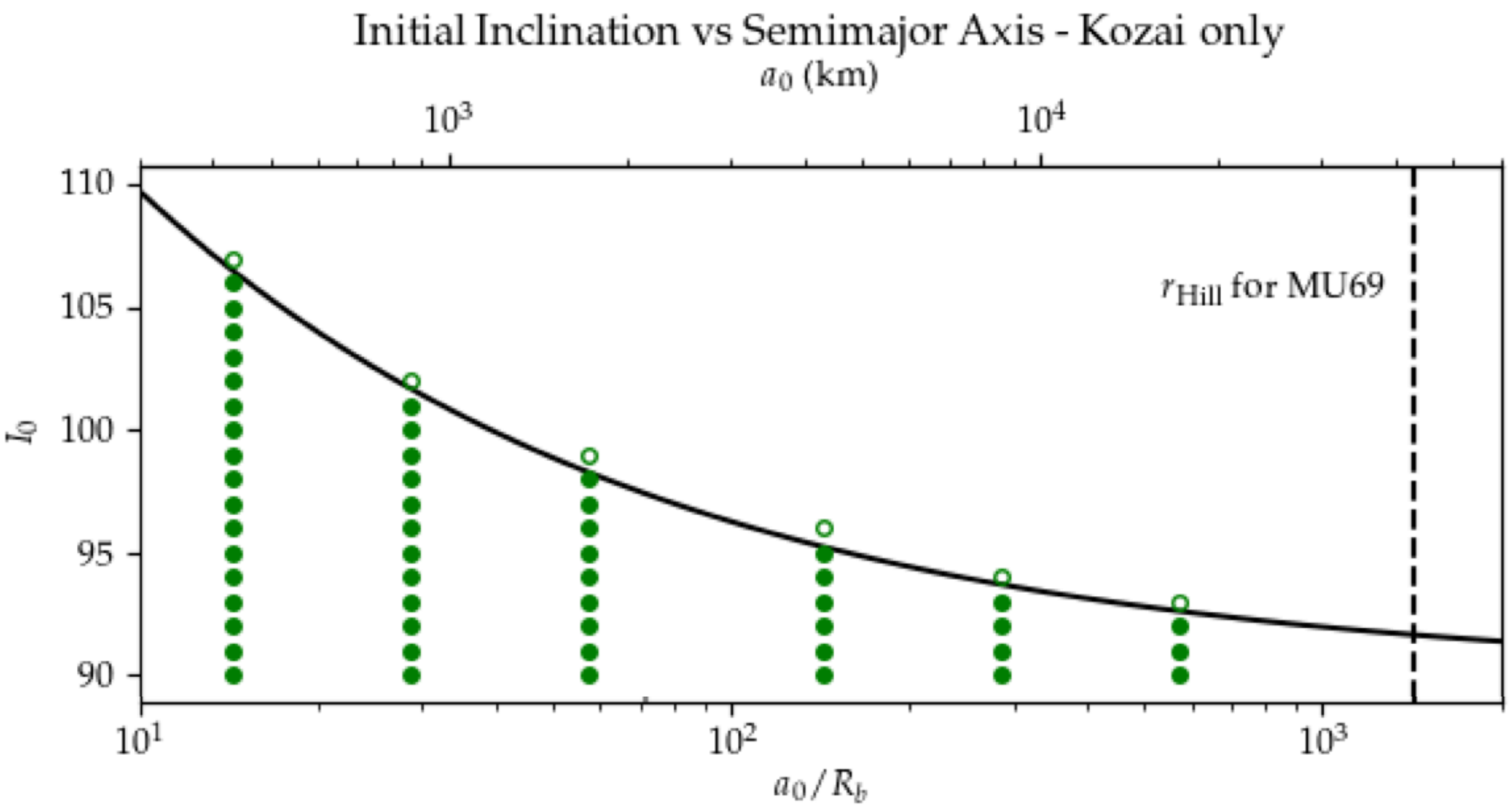

Lyra, Youdin, & Johansen 2020 (submitted)

Kozai + Tidal Friction + Drag

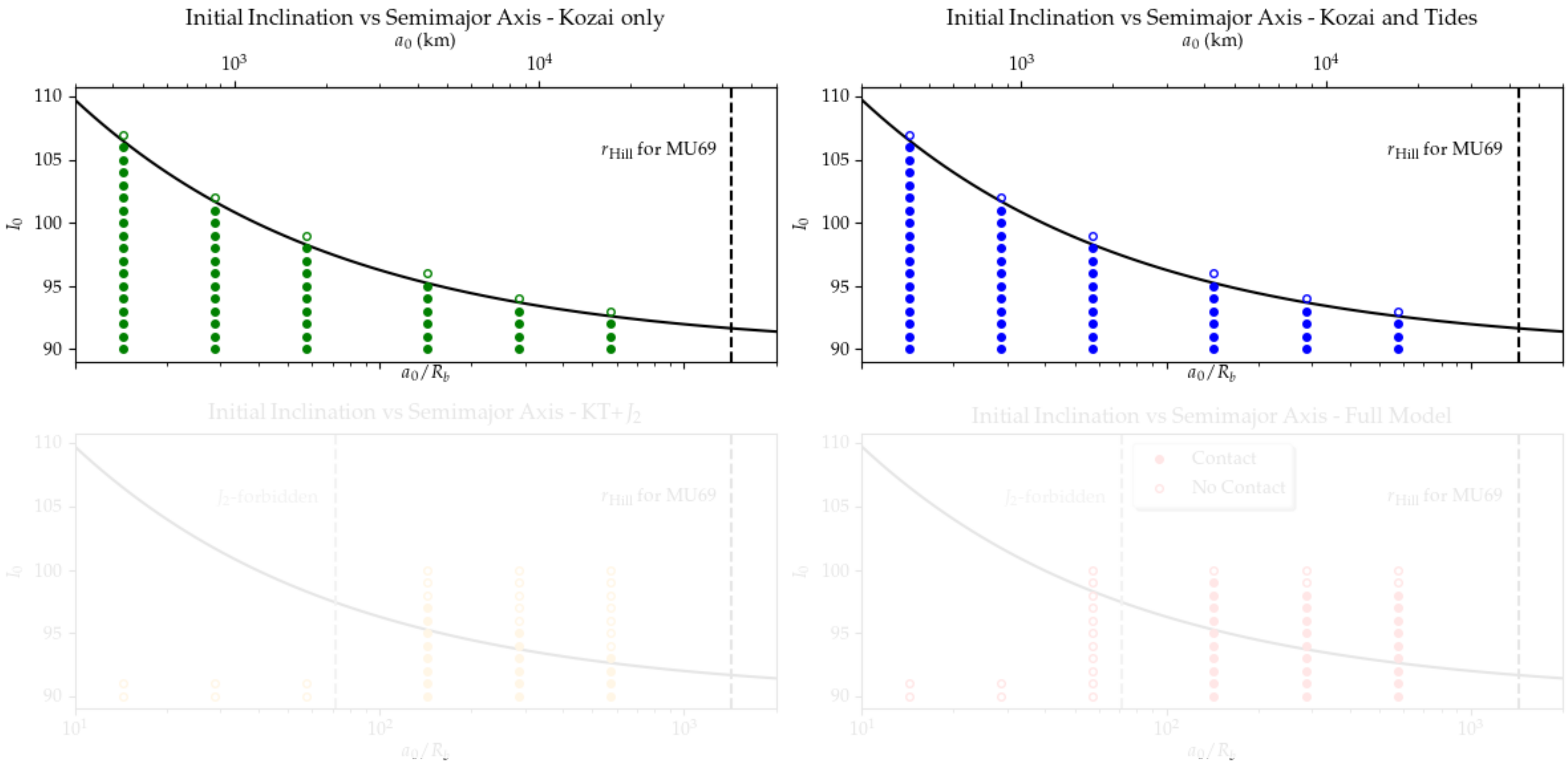

Lyra, Youdin, & Johansen 2020 (submitted)

Kozai + Tidal Friction + Drag

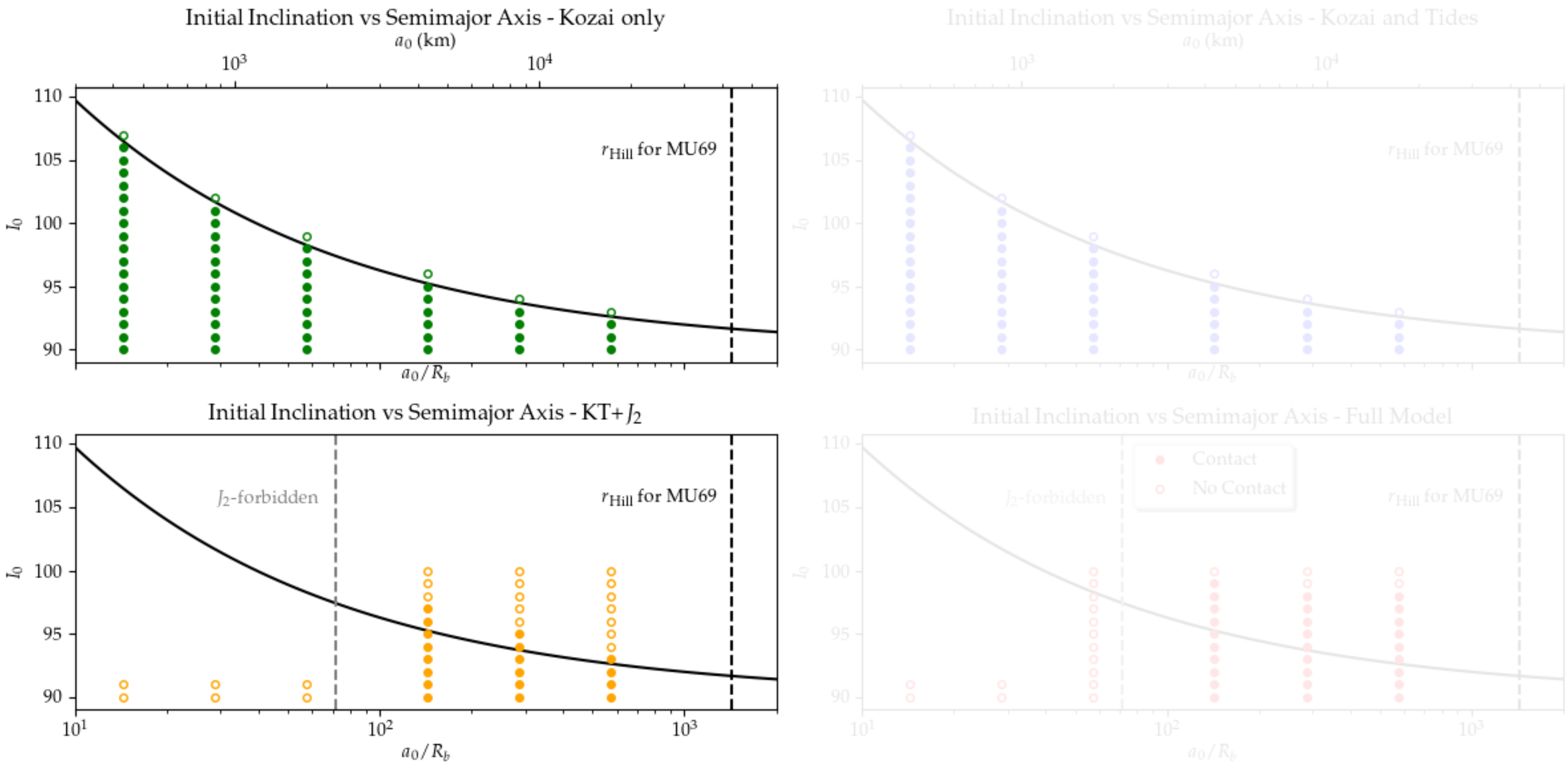

Lyra, Youdin, & Johansen 2020 (submitted)

Kozai + Tidal Friction + Drag

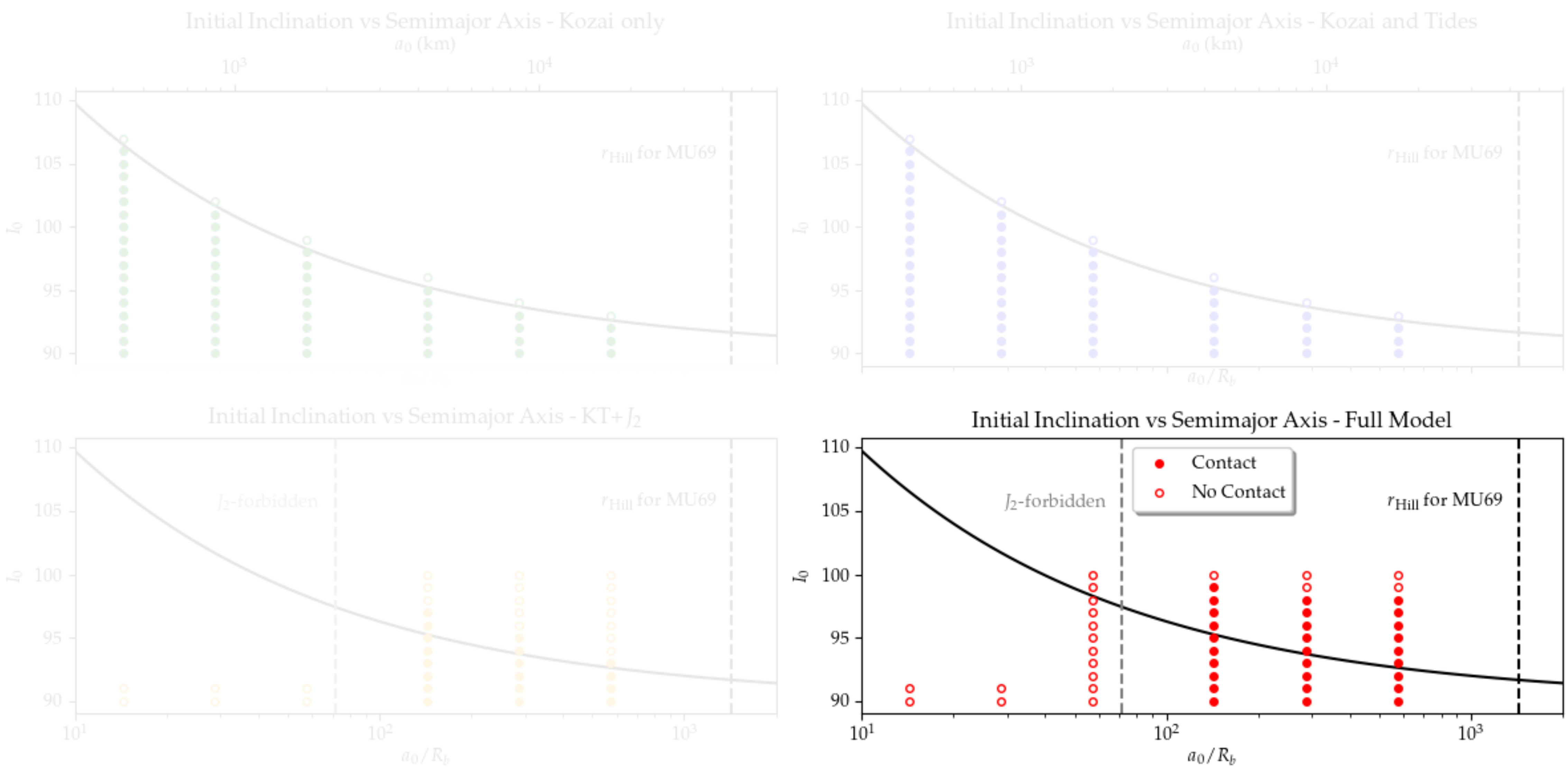

Lyra, Youdin, & Johansen 2020 (submitted)

Effect of Drag

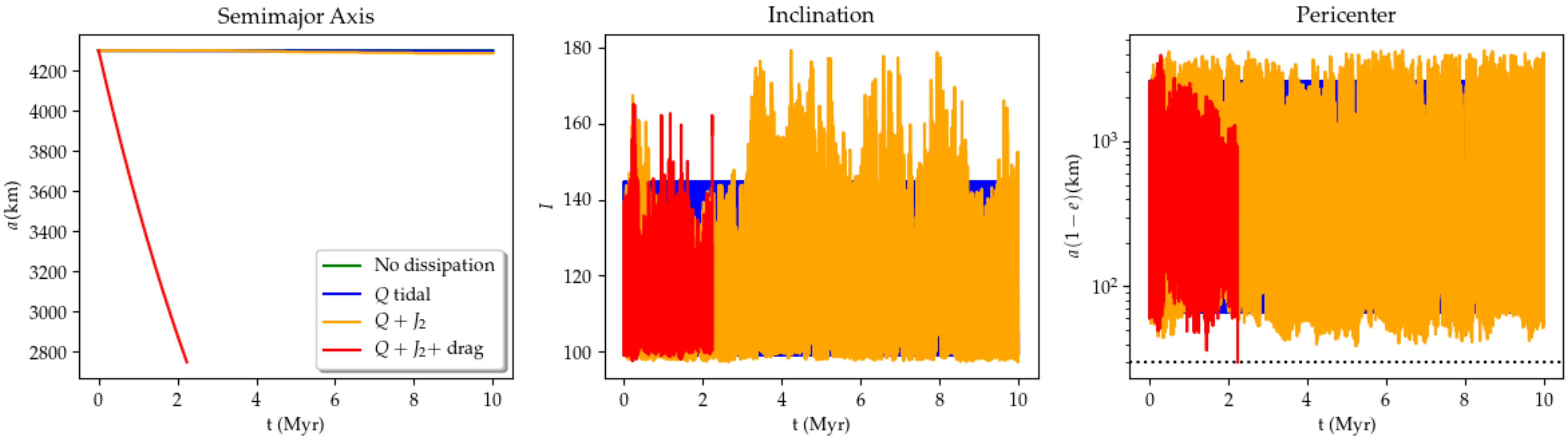

Lyra, Youdin, & Johansen 2020 (submitted)

Alignment of the Spin Vectors

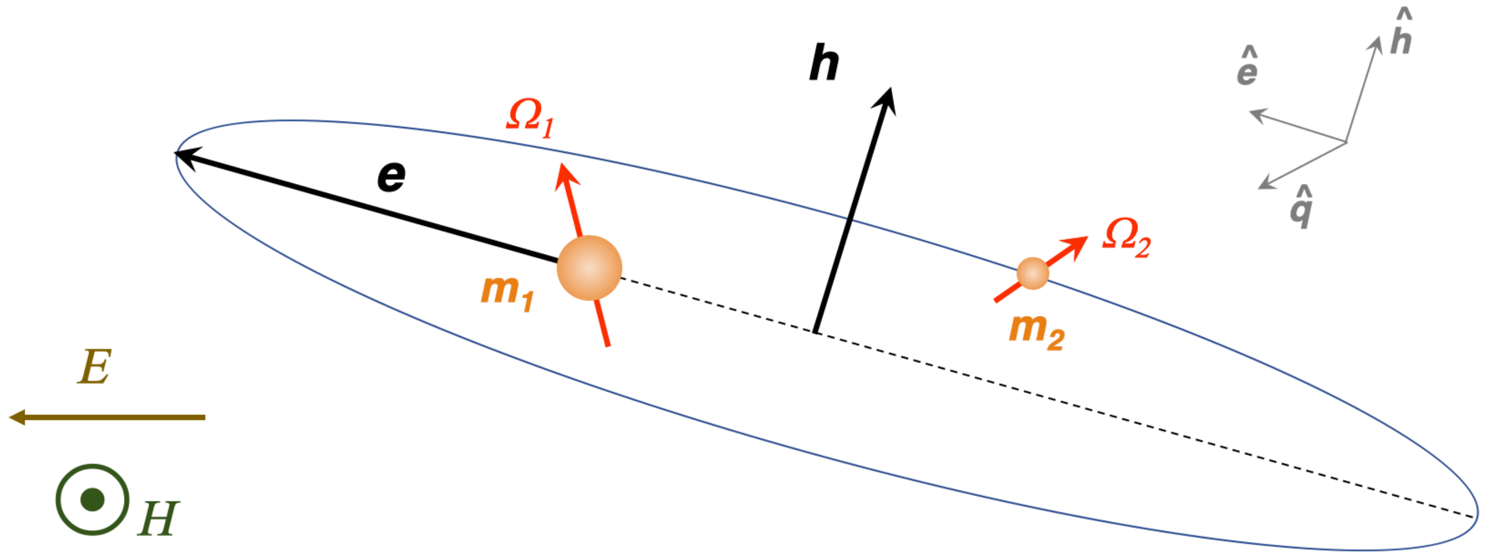

Mainly driven by J_2 (permanent quadrupole)

Timescale proportional to a^4 *(4^{th} power of semimajor axis)*

5 Gyr for $a/R \sim 100$

0.5 Myr for $a/R \sim 10$

Lyra, Youdin, & Johansen 2020 (submitted)

Fine Tuning of Initial Inclination

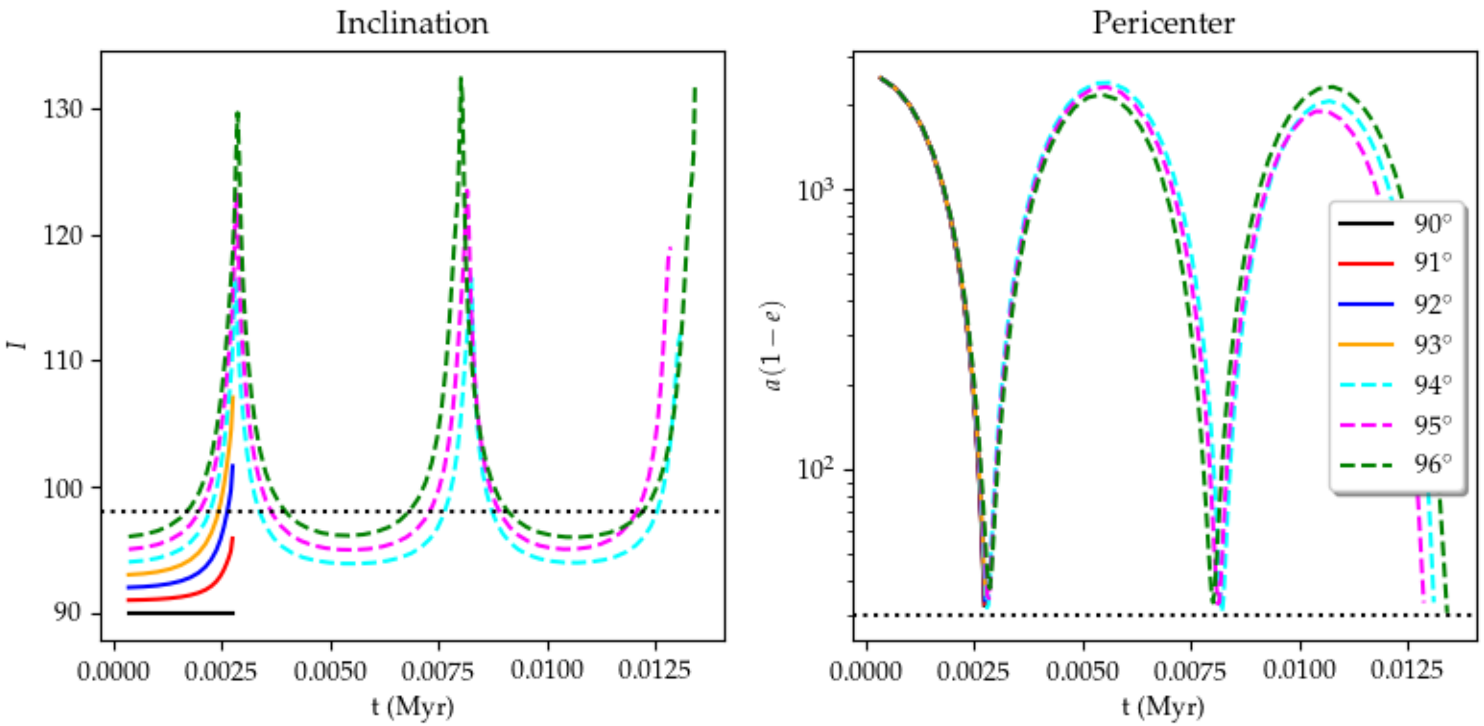

Double-Averaged vs Single-Averaged

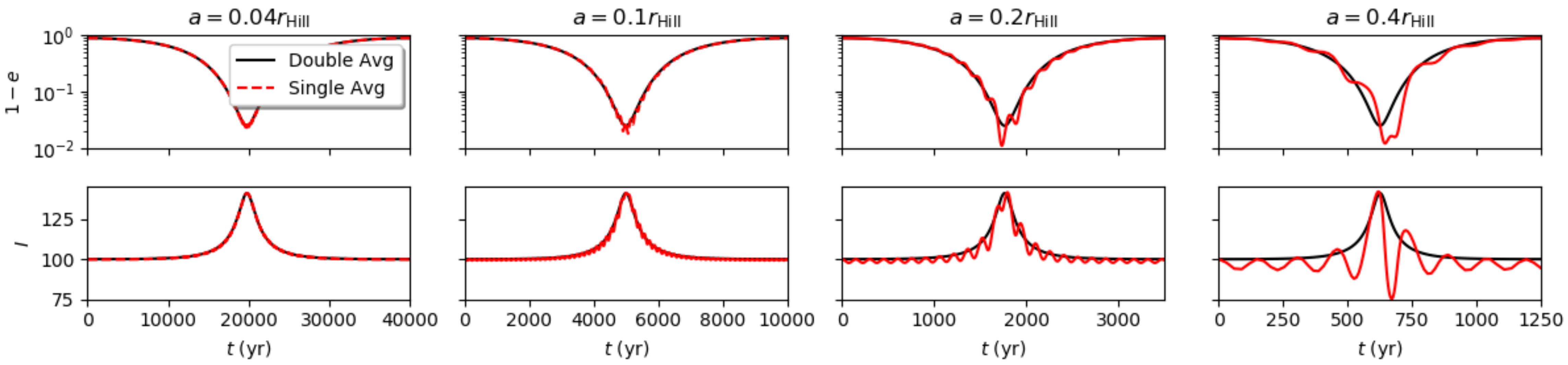

Lyra, Youdin, & Johansen 2020 (submitted)

N-body simulations (no tides, J2, or drag)

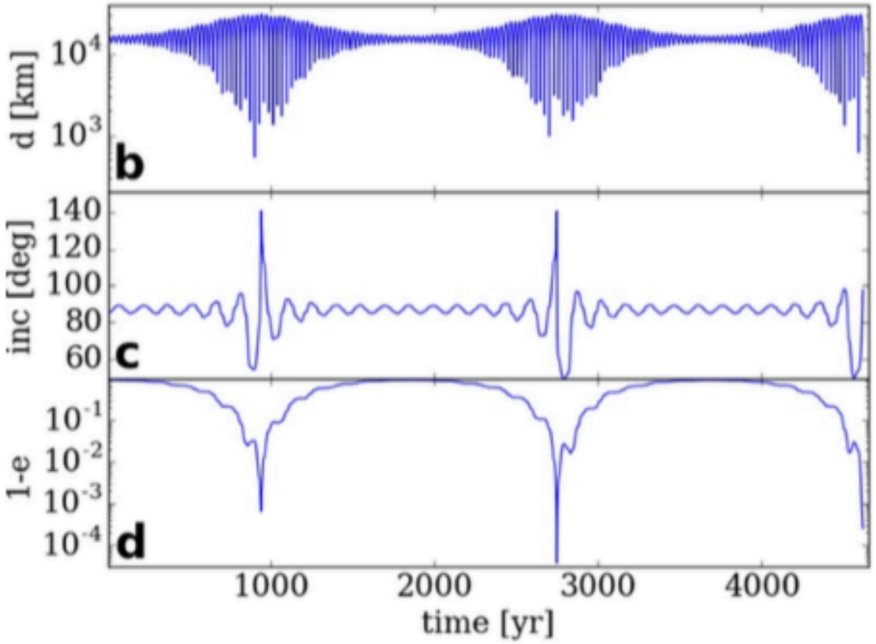

Inclination not limited to the double-averaged constraint.
Cycles lead to lower inclination than initial.
Prograde/retrograde flipping possible.

Grishin et al. (2020)

N-body simulations (no tides, J2, or drag)

Pericenter

Time to contact

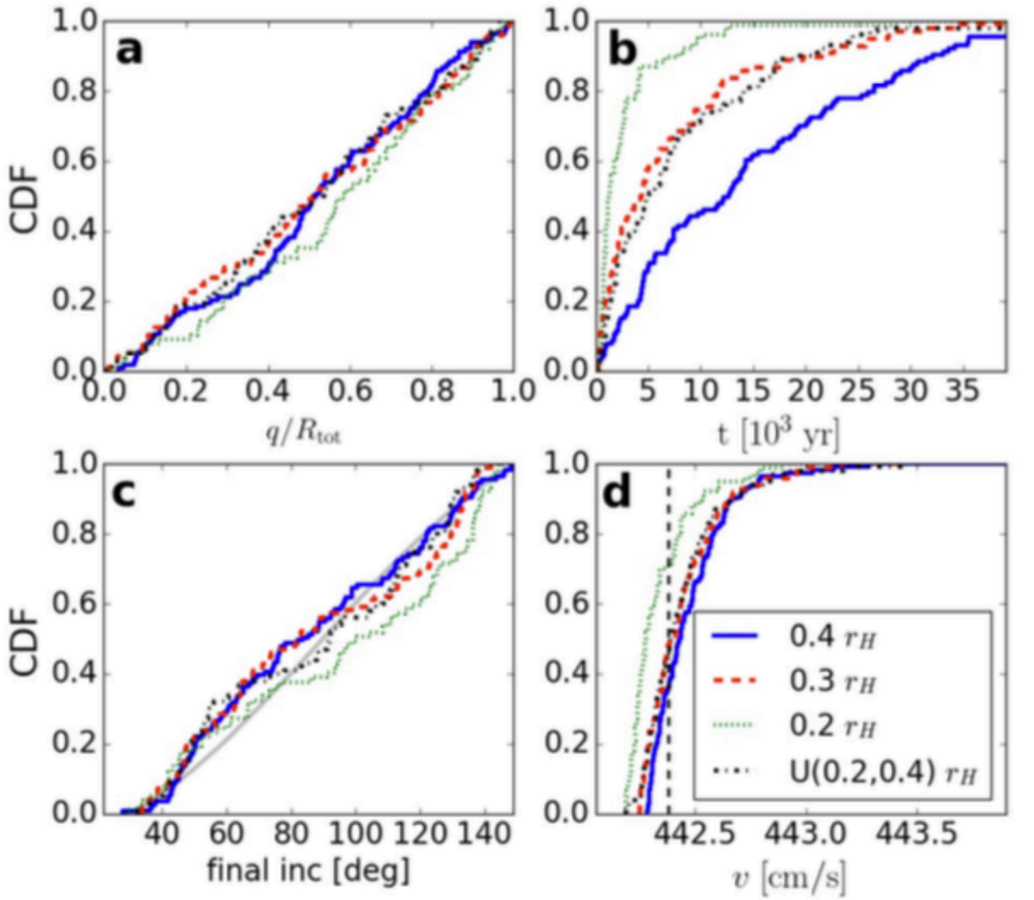

Inclination at contact

Speed at contact

Grishin et al. (2020)

N-body simulations (no tides, J2, or drag)

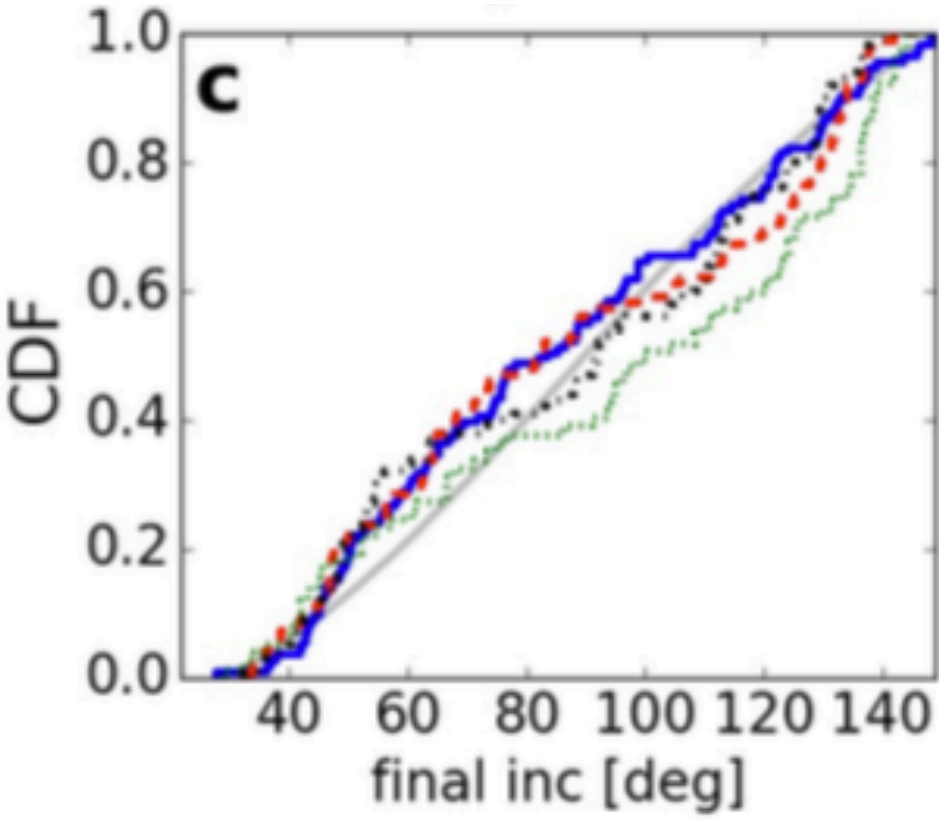

Inclination at contact

Uniform
any inclination (from 40^{o} to 140^{o}) equally likely

Grishin et al. (2020)

N-body simulations (no tides, J2, or drag)

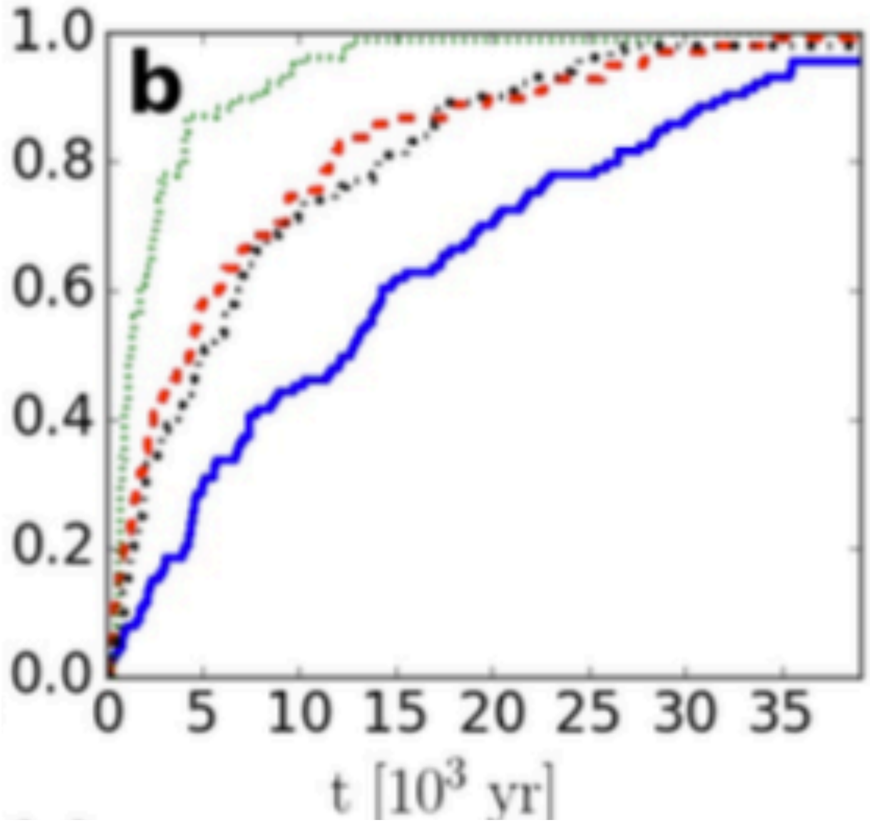

Time to contact

Too short to allow for alignment

Grishin et al. (2020)

Conclusions

- Solved the binary planetesimal problem with gas drag
- Implemented the solution into a Kozai plus tidal friction code
- Contact possible in the asteroid belt within 0.1 Myr (depleted of binaries)
- Contact via Kozai cycles in the Kuiper belt, orbits become grazing
- Window of contact increased by J_2 and drag
- Enough time for the bodies to come to alignment
- Model predictions:
  - ~ 10% of KBCC binaries should be contact binaries
  - Velocities at contact should be about 3-4 m/s
- Open questions:
  - Single-averaged (or N-body) needed to reproduce final inclinations
  - Combine our model with single-averaged Kozai (or N-body)

...1 January 2019.

The two bodies slowly spiral closer until they touch, forming the bi-lobed object we see today.

Sketch by J.T. Keane

Lyra, Youdin, & Johansen 2020 (submitted)

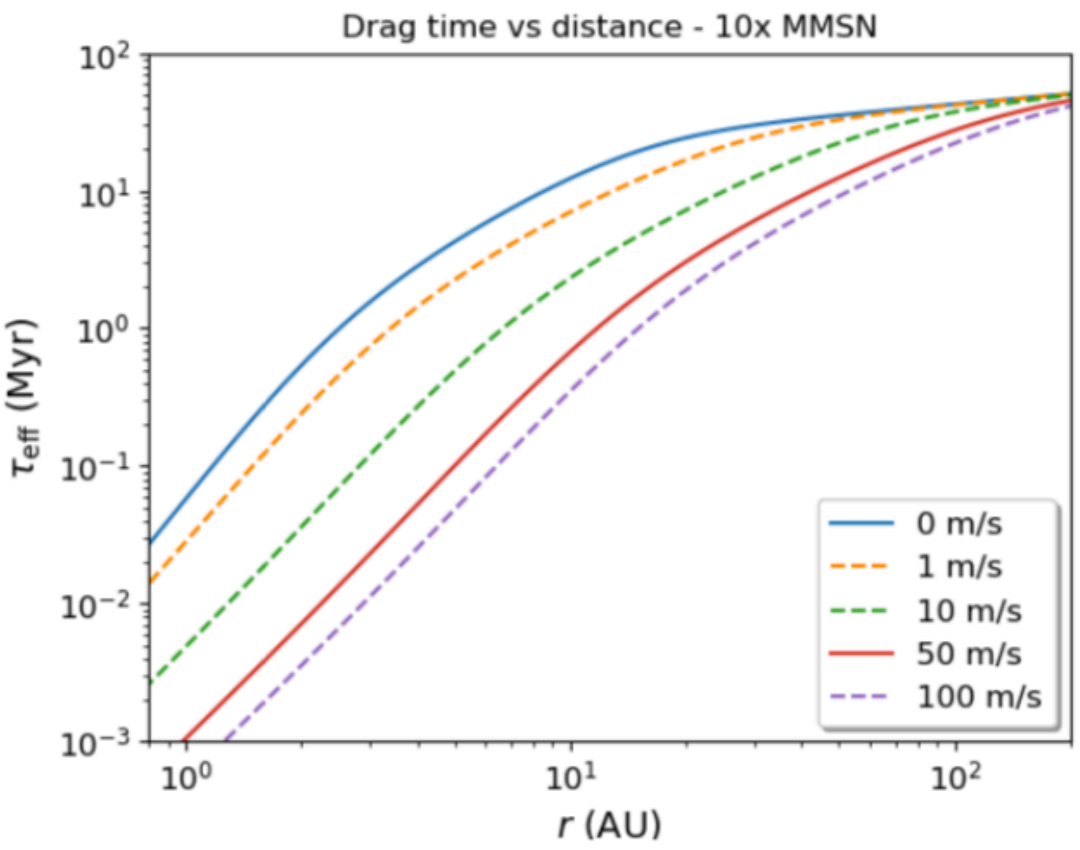

Drag time vs distance - 10x MMSN
τ_{eff} (Myr)
r (AU)
0 m/s
1 m/s
10 m/s
50 m/s
100 m/s

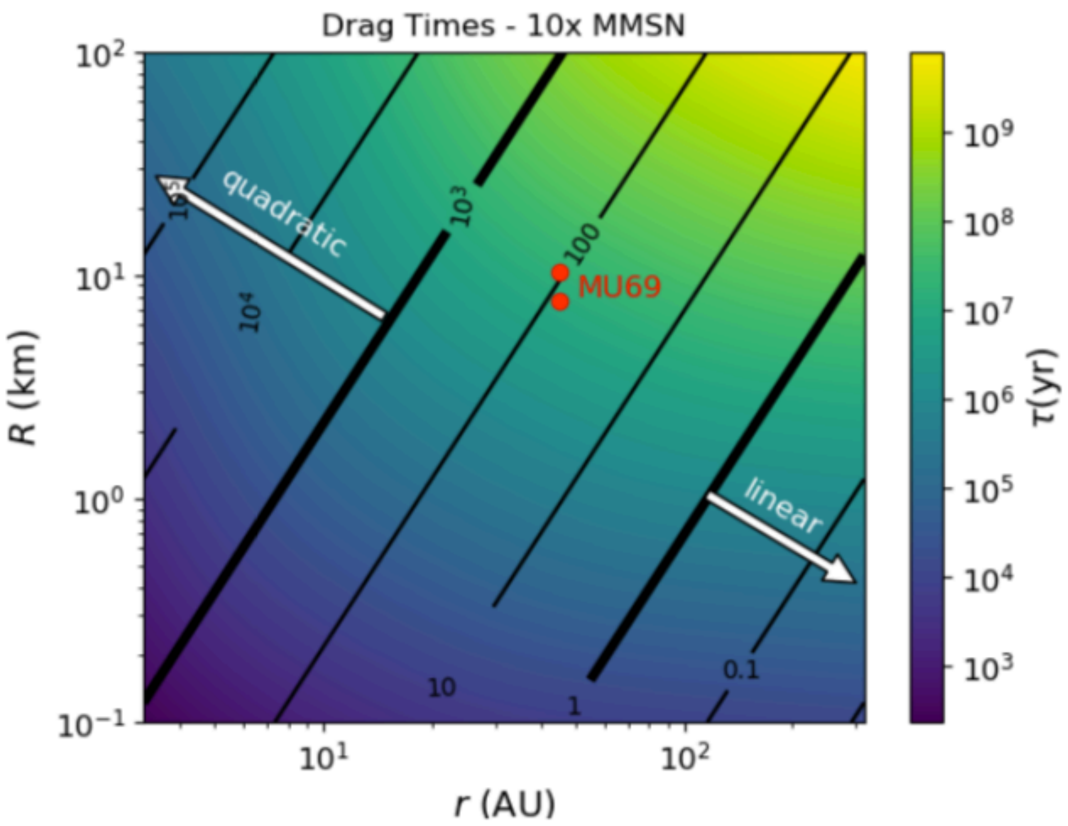

Drag Times - 10x MMSN
R (km)
r (AU)
τ(yr)
quadratic
linear
MU69
10^3
100
10^4
10
1
0.1

Sputnik Planitia – N_2 frost

MU69 and Pluto ices are different

MU69 : Methanol, HCN, H_2O (?)

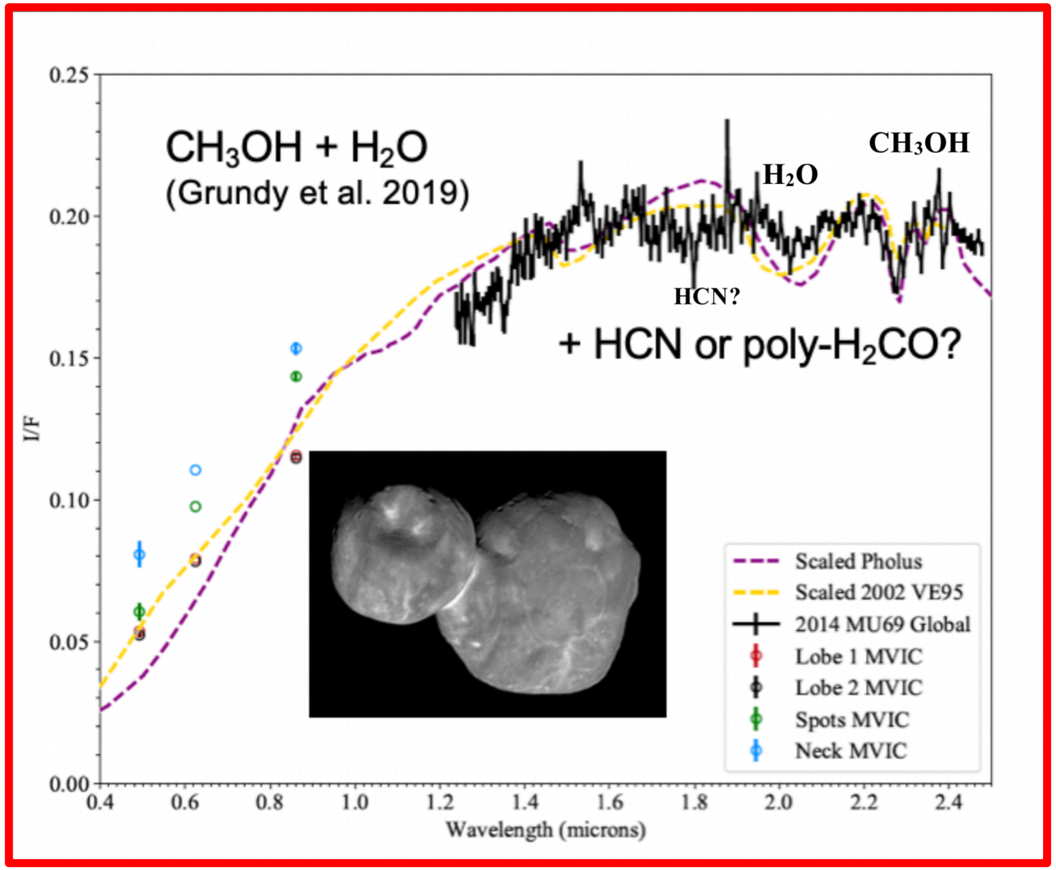

Pluto : CH_4, N_2, CO

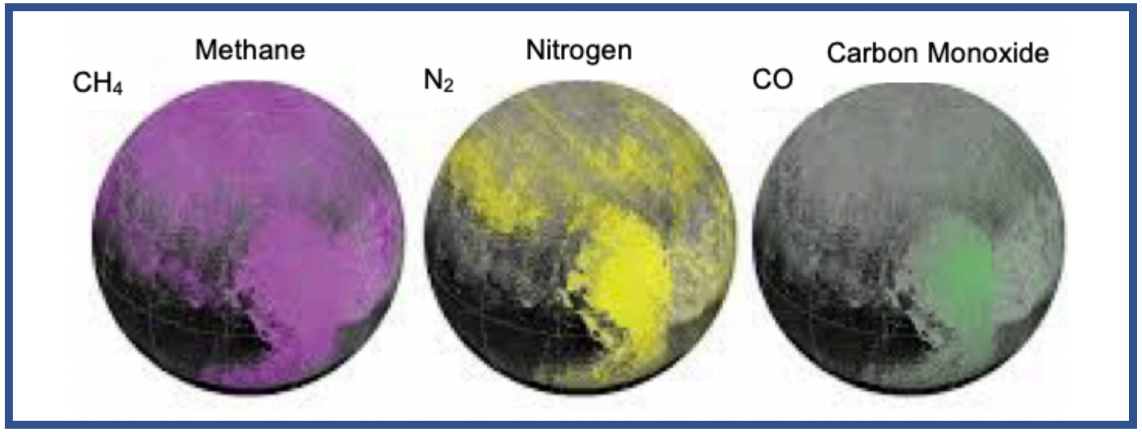

Grundy+ ’16, Lisse+ ’20, Grundy+’ 20

Retention of volatiles

If Pluto is formed from similar bodies to MU69, they must retain N_2

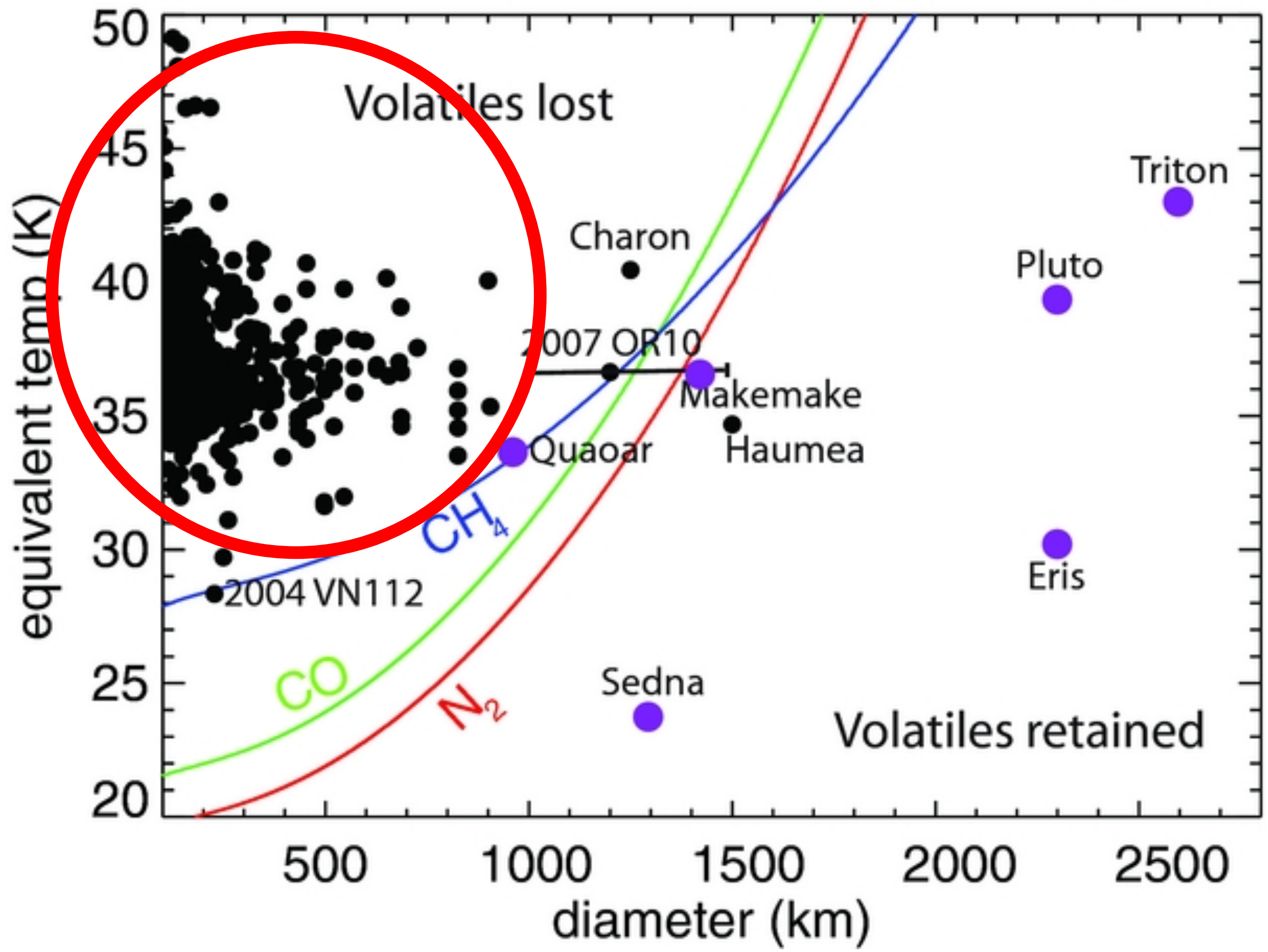

Needs shielding from sunlight

W. Lyra

Brown, Burgasser, & Fraser (2011); Lisse+ ‘20

Retention of volatiles

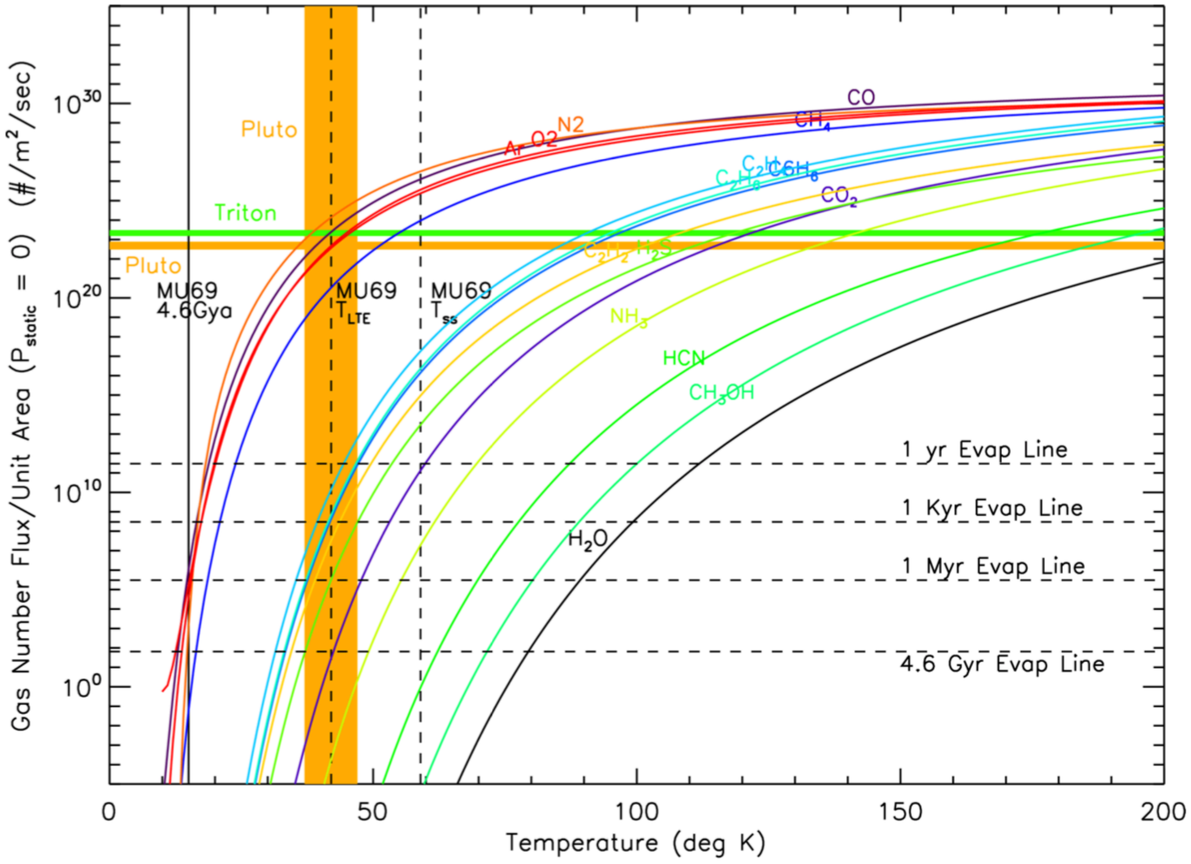

Hypervolatiles (CH_4 / CO / N_2)
lost under vacuum pressure and microgravity in ~1 Myr
for 40 K

Retained for long times if formed < 20K

Formation of MU69 in an optically thick disk keeps the interior cold enough to allow the volatiles to remain frozen.

Lisse+'20

Hardening during disk lifetime

For unequal mass the physics is similar, the
drag time is just replaced by an effective drag time:

Effective drag time

$$\tau_{\text{eff}} = (m_1 + m_2)\frac{\tau_1\tau_2}{\tau_2 m_2 + \tau_1 m_1}.$$

Exponential decay of angular momentum

$$h = h_0 e^{-t/\tau_{\text{eff}}}.$$

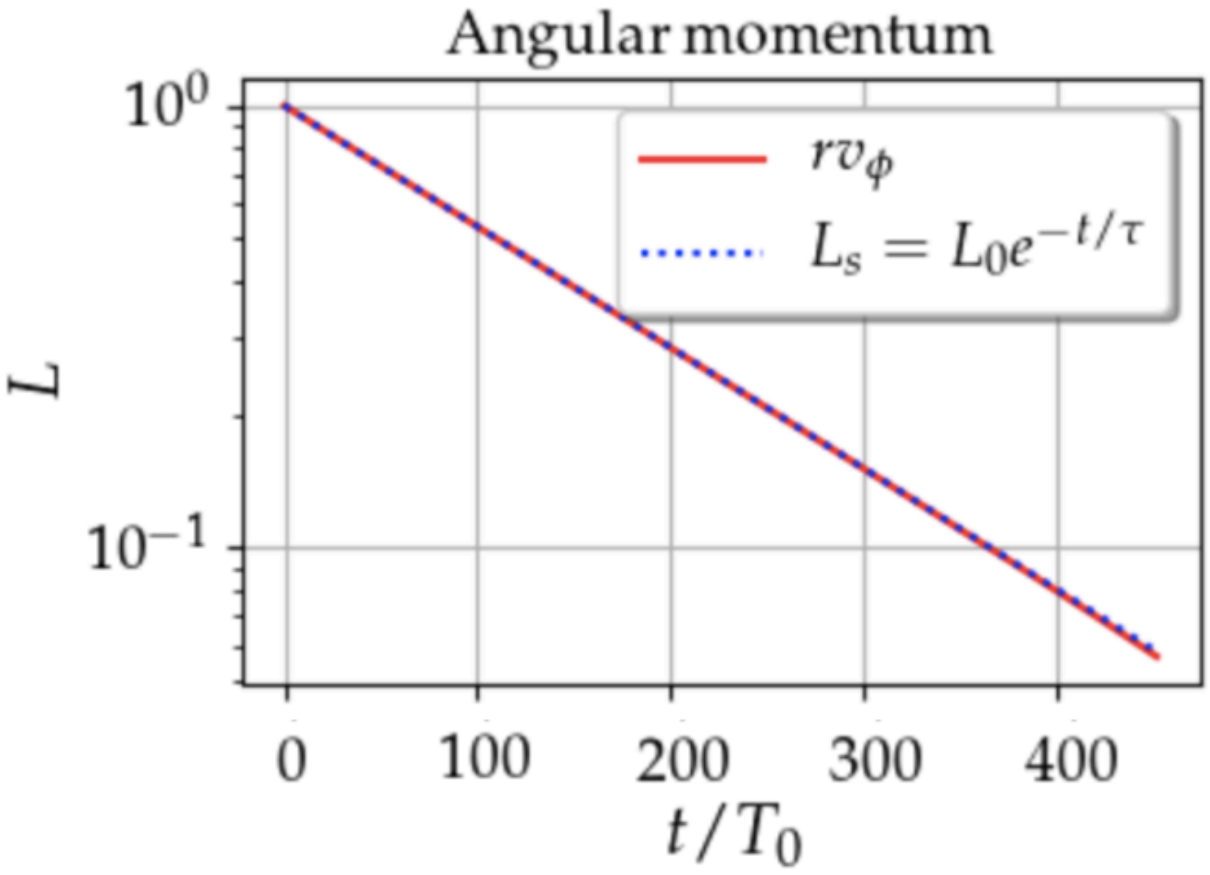

Lyra, Youdin, & Johansen 2020 (submitted)

Wind solution

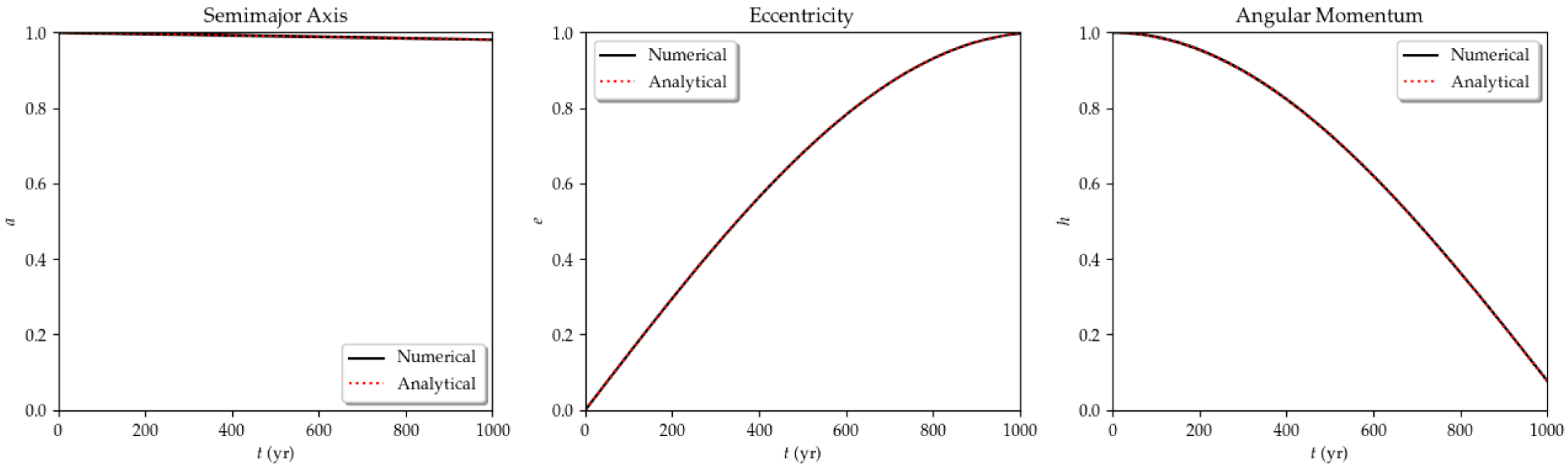

$$\langle a(t)\rangle = a_0 e^{-2t/\tau}$$

$$\langle e(t)\rangle = \cos\left[\cos^{-1} e_0 + \frac{3u}{2}\sqrt{\frac{a_0}{\mu}}\left(1-e^{-t/\tau}\right)\right]$$

$$\langle h(t)\rangle = e^{-t/\tau}\left\{h_0 - 1 + \cos\left[\frac{3}{2}a_0 u\left(1-e^{-t/\tau}\right)\right]\right\}$$

Lyra, Youdin, & Johansen 2020 (submitted)

Kozai-Lidov Oscillations

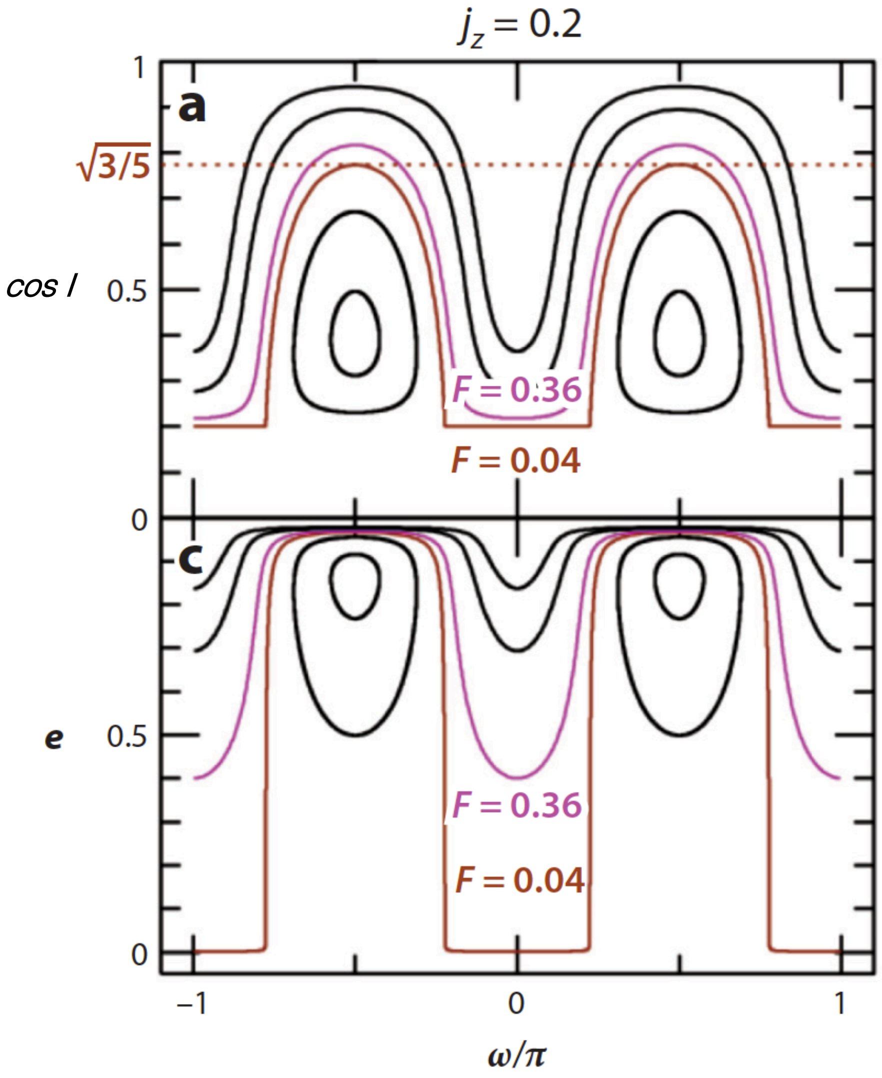

Conserved quantity is not angular momentum, but vertical angular momentum

$$j_z = (1-e^2)^{1/2} \cos I$$

Cycles of inclination and eccentricity.

Naoz 2016

Kozai-Lidov Oscillations

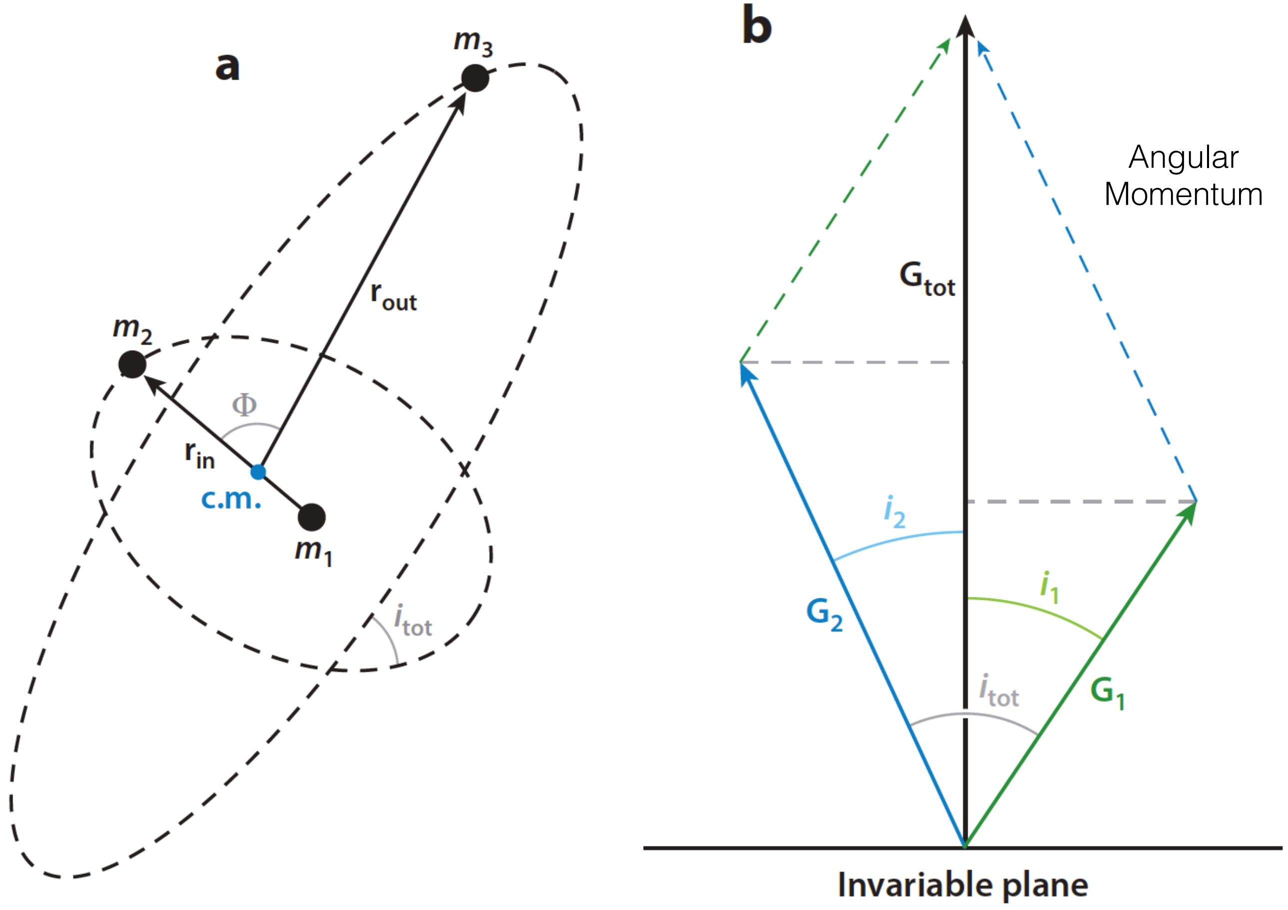

Conserved quantity is not angular momentum, but vertical angular momentum

$$j_z = (1\text{-}e^2)^{1/2} \cos I$$

Naoz 2016

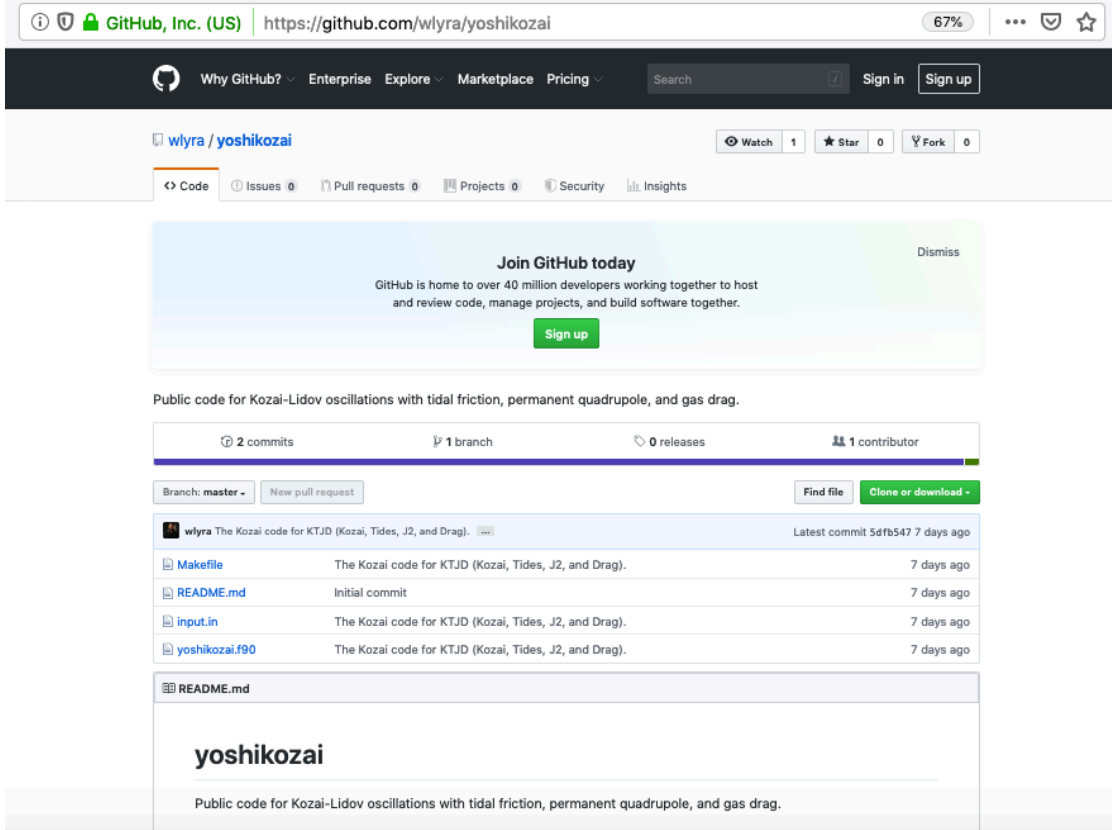

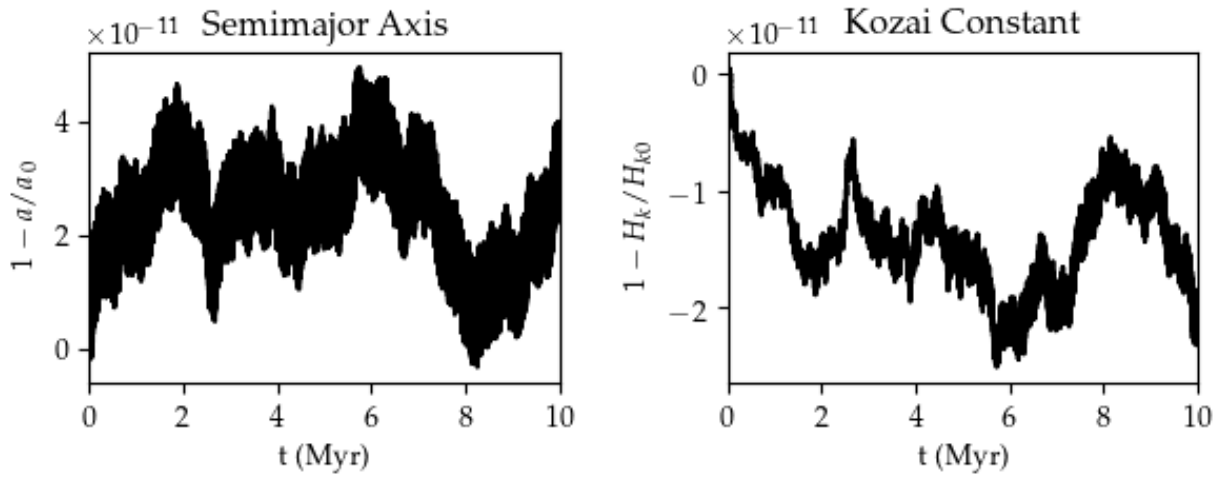

Lyra, Youdin, & Johansen 2020 (submitted)

Kozai + Tidal Friction + Drag

$$\frac{de}{dt} = -e\left[V_1 + V_2 + V_d + 5\left(1-e^2\right)S_{eq}\right],$$
$$\frac{dh}{dt} = -h\left(W_1 + W_2 + W_d - 5e^2 S_{eq}\right),$$
$$\frac{d\hat{e}}{dt} = \left[Z_1 + Z_2 + \left(1-e^2\right)\left(4S_{ee} - S_{qq}\right)\right]\hat{q} - \left[Y_1 + Y_2 + \left(1-e^2\right)S_{qh}\right]\hat{h},$$
$$\frac{d\hat{h}}{dt} = \left[Y_1 + Y_2 + \left(1-e^2\right)S_{qh}\right]\hat{e} - \left[X_1 + X_2 + \left(4e^2+1\right)S_{eh}\right]\hat{q},$$
$$\frac{d\boldsymbol{\Omega}_1}{dt} = \frac{\mu_r h}{I_1}\left(-Y_1\hat{e} + X_1\hat{q} + W_1\hat{h}\right),$$
$$\frac{d\boldsymbol{\Omega}_2}{dt} = \frac{\mu_r h}{I_2}\left(-Y_2\hat{e} + X_2\hat{q} + W_2\hat{h}\right).$$

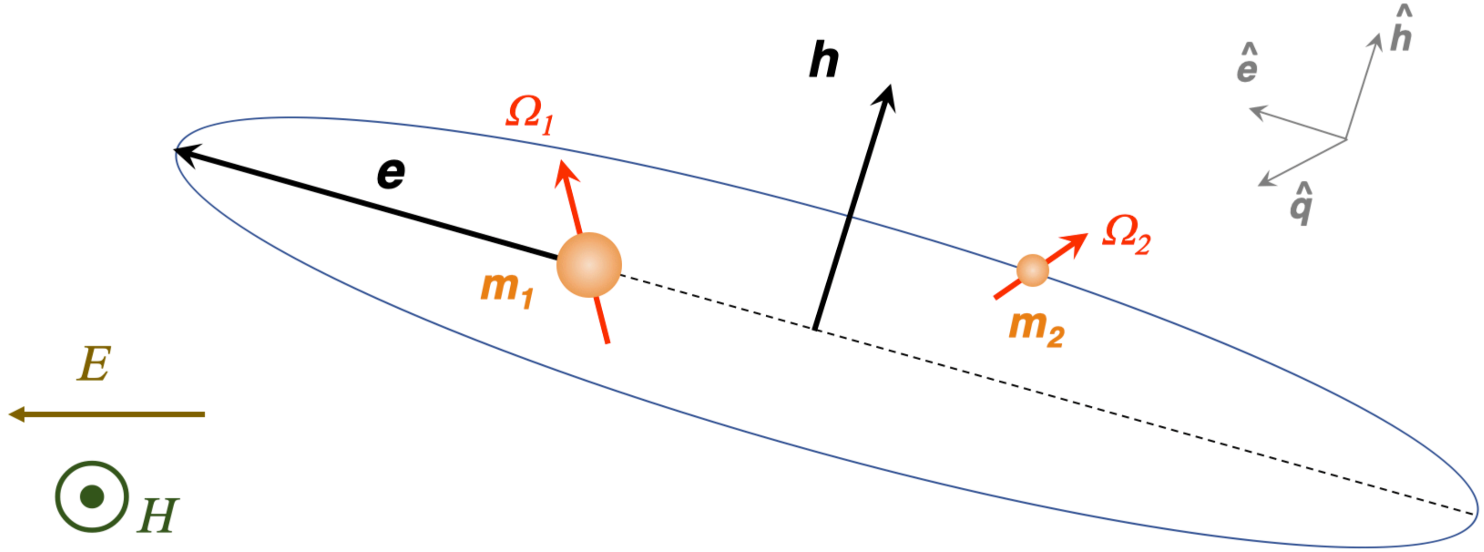

Lyra, Youdin, & Johansen 2020 (submitted)